SISSA - SCUOLA INTERNAZIONALE SUPERIORE DI STUDI AVANZATI
TRIESTE
Strada Costiera 11

ISAS - INTERNATIONAL SCHOOL FOR ADVANCED STUDIES

MHD JETS

Thesis Submitted for the degree of "Magister of Philosophiae"

Astrophysics Sector

Candidate:

Andrea Mason

Supervisor:

Prof. D.W. Sciama

Academic Year 1989/90

TRIESTE

Acknowledgements

...with a little help of my friends ...

Contents

Introduction

This study responds to the necessity of having a sort of tool-kit to investigate the jet phenomenon in astrophysics. Historically jets where first predicted theoretically and then shown to exist in extragalactic radio sources as a 'natural' way to take out energy from a central core and to deposit it far away ($\gg 100\,\mathrm{kpc}$). What we observe in extragalactic radio sources is mainly energy coming from two well separated regions which is radiated through non thermal incoherent synchrotron emission. The energy lost in the transport mechanism (jet) is negligible in comparison with the total energy of the source (typically $10^{58-60}\mathrm{ergs}$). This is also the main reason why jets where discovered later. Nowadays jets are common features in active galactic nuclei, in stellar contexts (*i.e.* $SS433$), and recently jet-like features have been found also in the supernova $SN1987a$. Here we focus our attention on jets in extragalactic radio sources, just because much work it has been done in this direction from a theoretical point of view and observationally.

As we said, jets connect two regions: a compact region (the core – parsec scale) located at the center of the AGN and a more extended region (radio lobe – 10 - 100 kpc scale) where most of the energy emitted comes from. The need for an "efficient" engine to release energy which is channelled and flowing out to such distances is clear. The most widely used engine model is constituted by

a massive black hole (typically 10^8 solar masses) where the outflow of material (jet) is a by-product of an accretion process. We will not discuss how jets are formed, instead we simply assume their existence.

The title, MHD Jets, reflects the conviction, that we are dealing basically with phenomena concerning outflow of plasmas traversing a magnetized atmosphere where the magnetic field affects its structure, dynamics and radiative properties.

The plan of the work is a sort of itinerary, from simplicity to complexity, starting with a phenomenological discussion about jets, with some models (fluid models) proposed initially. Then the deficiencies of these models are partly recovered by magnetohydrodynamical models (MHD models) which include some fundamental processes occurring in a magnetized plasma, which are known to be present for example in the solar wind (MHD instability and MHD turbulence). The last chapter addresses two problems concerning the interaction of a jet with its ambient. In our view this is really where jets are useful (if they are well interpreted), to understand the physical conditions of the medium traversed by them. The mathematical analysis does not always gives analytic solutions to these problems. In particular it involves the description of small scales plasma turbulence which produces structures that are not resolvable observationally yet.

1. Relevance of Radio Jets in Extragalactic Sources

1.1 Preliminary Remarks

Since the word "jets" was first used from the extragalactic astronomers to describe elongated luminous features,[1] a "jet language" permeates the optical, radio and X-ray literature. Observationally, jets are thin features that connects two different regions of emission. They emanate from a nucleus and end in a more extended region and are interpreted as paths of fluid outflows. The large sizes of powerful extragalactic sources show that active galaxies and QSRs eject *something* that can supply energy to relativistic particles and magnetic fields to regions separeted from the nucleus.

In the early 1970's, the existence of elongated kiloparsec-scale optical and radio features in a few bright sources encouraged continuous flow, or "beam", models of energy transport. The principal aspects of these models can be summarized as follows:

- No adiabatic losses, since the bulk kinetic energy in a beam exerts no pressure.
- Supersonic beams terminate at shocks near their interface with ambient gas. Shocks can transform beamed kinetic energy into relativistic particle

1 Baade and Minkowski (1954) made the first use of the word jet in an extragalactic context to interpret the optical knots in M87 as an outflow from the nucleus.

and field energy, thus providing a framework for explaining the locations, brightness distributions, and short radiative timescales of hot spots in radio lobes.

These attractions of the "beam" models are such that observers now use the word "jet" as a synonym for "elongated feature" mainly because they find such features in places where beam models postulate continuous collimated outflow, not because they have direct evidence for the outflow itself.

The current state of the observations of extragalactic jets is summarized by Bridle and Perely (1984). The current state of the theory is reviewed by Begelman, Blandford, and Rees (1984).

Stellar jets, or "bipolar flows", have a much better identification than this, as outflow velocities have been directly measured in many cases. In SS433, the radio proper motions and optical spectroscopic data both show a mean velocity of 0.26c, and the flow geometry is known in detail. The $\sim$ 100 light-day scale and typical 1.4 GHz luminosity of SS433 ($P_{tot}^{1.4} = 10^{15.8}$ W/Hz) are much less than those of extragalactic jets. There is also good evidence for collimated outflow from recently formed stars – velocities of tens to hundred of km/s are known from Doppler shifted molecular emission lines at mm wavelengths, from optical spectroscopy of nearby Herbig-Halo objects, and from the 2.12 μm line of H_2. It is not clear, however, that the processes which produce these galactic jets scale to the extragalactic case.[2] They nevertheless show that supersonic jets can arise in astrophysical situations where accretion flows and disk geometries may be relevant.

2 They may allow us to study the propagation and stability of supersonic jets in a background medium with measurable properties, thus becoming a "laboratory test" of models of jet dynamics (though possibly not in the same regimes of Mach number, density contrast, or Reynolds number as in the extragalactic case).

1.2 Definition of Jet

We need clear morphological criteria in order to define a feature as "jet". Three criteria have been used (Bridle 1982; Bridle and Perley 1984, BP):

(*a*) a radio feature must be at least four times as long as it is wide,

(*b*) separable at high resolution from other extended structure (if any) either by brightness contrast or spatially,

(*c*) aligned with the radio core where it is closest to it. This is to distinguish *jets* from misaligned ridges near the hot spots in radio lobes.[3]

Even these three seemingly simple criteria are not always easy to apply. For example, the jet in NGC6251 (Perley *et al.* 1984) could be defined as a train of discrete knots, and not all are aligned, if we observe it with a lower sensitivity to smooth emission. Such trains of knots could be called *jets* only if some knots are elongated along the length of the train, or if it comprises more than two knots, as in 3C219 (figure 1).

If we apply criterion (a) strictly, we may exclude some real blobby jets. Furthermore, often we observe a faint emission, "cocoons", around jets, (see sources like M84 and 3C341), so that the distinction between faint cocoons from brighter jets is not simple when discussing jet properties. Infact the collimation properties of the cocoons in M84 and 3C341 are quite different from those in jets; in these cases the distinction is not purely semantic. Therefore the study of jets has to diagnose the relationship between jets and other 'very similar' structures. For instance: are the cocoons faint "outer jets", leakage from the jets, or emission from the backflows predicted by numerical simulations of hypersonic jet propagation in confining media?

3 These lobes features may be closely related to jets if there is redirected outflow beyond, or backflow from, the hot spots, but no interpretation of misaligned ridges in the lobes is yet obligatory and it is still useful to make empirical distinctions based on their alignment.

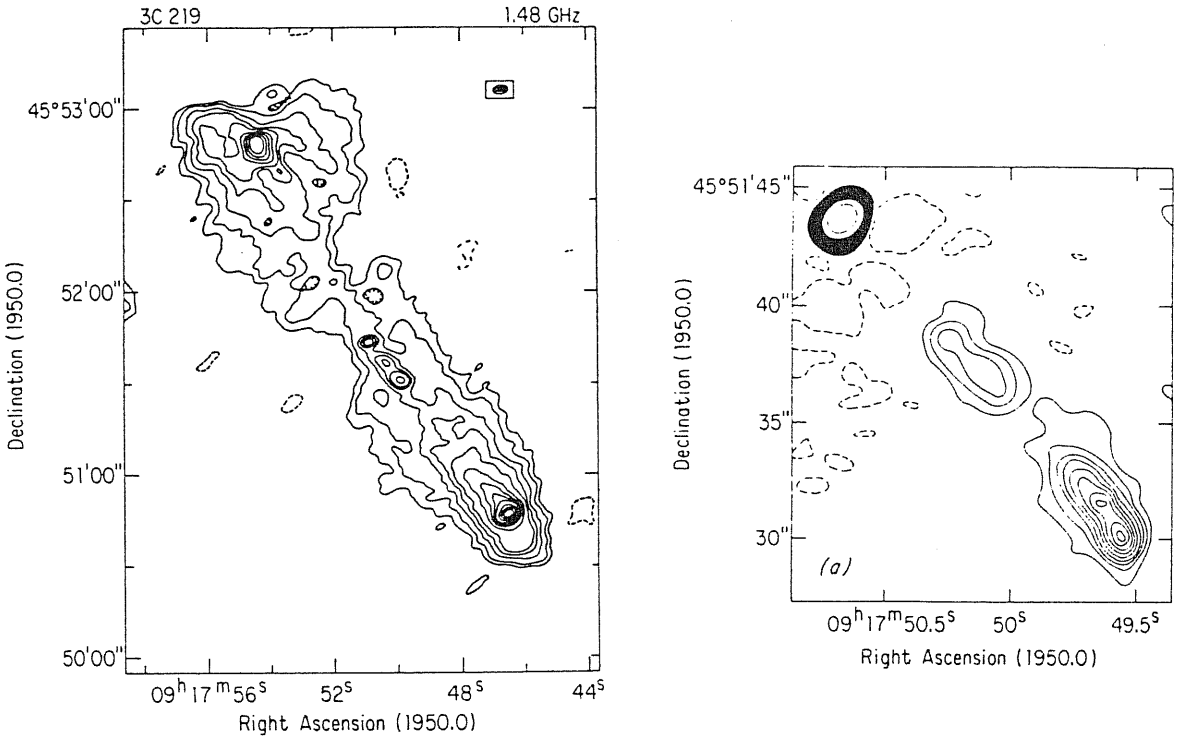

Figure 1: (Left panel) VLA 1465 MHz map of 3C219 with 1.7 arcsec resolution.Countours are plotted at -1,1,2,3,4,5,6,8,10,12,14,16,20,30,40 and 50 times 2 mJy per beam. (Right panel) VLA 4885 MHz map of a ~ 20 arcsec region near the nucleous of 3C219 at ~ 0.35 arcsec resolution. The brightest feature in the radio core. Note the elongated knot to the north-east of the core – presumably the brightest part of the counterjet, as it is elongated along the jet axis. Note also that this knot is opposite the end of the initial "gap" in the main jet.

Based on the above criteria, Bridle and Perley (1984, BP), have listed 125 extragalactic radio jets. The list is not statistically "complete" to a given flux-density limit, or in a given volume of space. However, it is the largest available catalog of jets in sources representing the entire $\sim 10^7 : 1$ range of total power associated with active extragalactic objects. It exhibits several trends that are unlikely to reflect statistical incompleteness or biases.

Jets occur in extragalactic sources of all luminosities, sizes and structure types, justifying the assumption that they are associated with processes common to all extragalactic radio sources. Every jet in the BP list is accompanied by a detectable radio "core" in the inner kpc of the parent object, though in some sources the cores are fainter than the brightest parts of the jet at cm wavelengths by factors ~ 2 to 4. This broadens the case for relating jets to continuing activity in the parent objects, supported further in some sources by the presence of VLBI jets. The fact that jets are neither rare nor confined to any one type of extragalactic source is strong support for the now-conventional assumption that they result from inefficiencies in the basic process of energy transport from the cores to the lobes. This conclusion is independent of whether the dissipation occurs in the primary flow itself, or in a backflow around it.

It is important, at this point, to identify what property of the sources changes with power and produces systematic trends in the properties of their jets. The properties to investigate are:

(*a*) *Sidedness*: it is related to the symmetry of the lobe of the powerful doubles radio sources that is strongly broken by their jets. The data of BP show that in weaker sources ($P^5_{core} \leq 10^{23-23.2}$ W/Hz or $P^{1.4}_{tot} \leq 10^{24.5}$ W/Hz) the kiloparsec scale jets have counter jets with more than 1/4 their brightness per unit length. They are called two-sided. Most kiloparsec jets in powerful sources, whether radio galaxies or QSRs, are one-sided (more than 4 : 1 in brightness) for their entire length, (figure 2).

There are few transitional cases, with $P^{1.4}_{tot} = 10^{24.5-25}$ W/Hz between large-scale two-sidedness and large-scale one-sidedness. This value of power marks also the transition between morphological classes I (edge darkened) and II (edge brightened) of Fanaroff and Riley (1974). The trend is clear: jets in weak, edge darkened sources are much more sym-

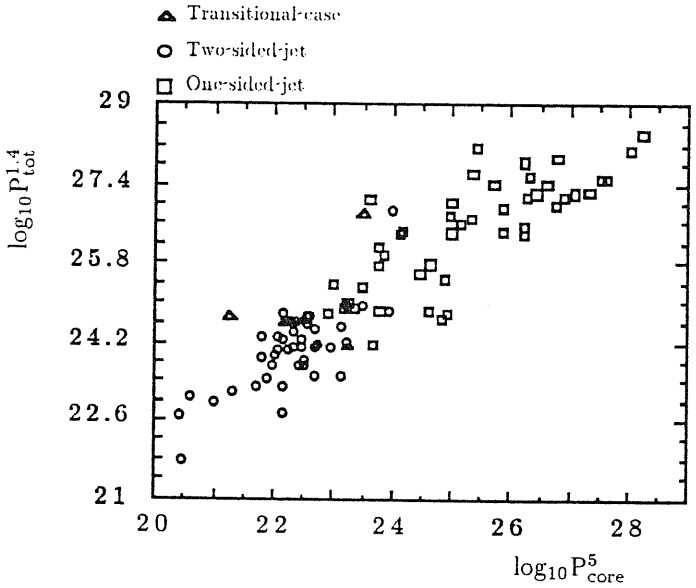

Figure 2: Distribution of the jet sidedness in the plane of logarithmic core power vs logarithmic total power; adapted from the data of Bridle, 1984.

metric on the large scale than those in powerful, edge brightened sources.

(*b*) *Magnetic Configuration*: there are three principal configurations of the apparent magnetic field $\mathbf{B}_a$. It denotes the direction of the magnetic field in a radio source inferred from observations of its linear polarization. Faraday rotation and depolarization are ignored: $\mathbf{B}_a$ is then at right angles to the E-vector of polarized radiation.

1. $B_{\parallel}$, *i.e.* $\mathbf{B}_a$ is predominantly parallel to the jet axis all across the jet.

2. $B_{\perp}$, *i.e.* $\mathbf{B}_a$ is predominantly perpendicular to the jet axis all across it.

3. $B_{\perp-\parallel}$, *i.e.* $\mathbf{B}_a$ is predominantly perpendicular to the jet axis at the center of the jet, but becomes parallel to the axis near one or both of its edges.

Of the 125 sources listed on BP, only for 40 the detailed polarimetry is

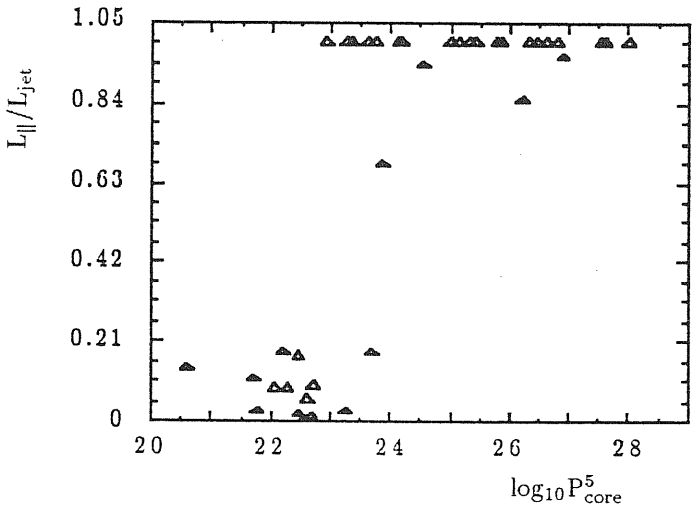

Figure 3: Change in dominant jet magnetic field configuration with increasing core power for about 40 sources. $L_{\parallel}$ is the length of the segment of the jet where the field is aligned predominantly parallel to the jet axis, L_j is the total length of the jet. Adapted from the data of Bridle, 1984.

available. Two-sided regions of straight jets have mainly, either the $B_{\perp}$ or the $B_{\perp-\parallel}$ configuration. Instead, one-sided regions have mainly the $B_{\parallel}$ configuration. Within the same jet the magnetic configuration can change along its length;[4] in straight jets emanating from weak cores, $\mathbf{B_a}$ usually turns from $B_{\parallel}$ to $B_{\perp}$ or $B_{\perp-\parallel}$ in the first 10% of their length, while jets associated with powerful cores are generally $B_{\parallel}$-dominated for their entire length, (figure 3).

The transition in magnetic properties occurs at $P^5_{core} = 10^{23-24}$ W/Hz (corresponding roughly to $P^{1.4}_{tot} = 10^{24-25}$ W/Hz). If we combine this with the sidedness trend, the Fanaroff-Riley classification, and the occurrence of

4 Treating jets as MHD fluids, the resistivity, for most of them, can be neglected and the magnetic field can be considered as frozen in the plasma. The magnetic flux is then conserved along the jet. Simple estimates of variation along the jet of the components $B_{\parallel}$ and $B_{\perp}$ follow, if one assume that the velocity is uniform over the cross-sectional area of the jet, $B_{\parallel} \propto R_j^{-2}$ and $B_{\perp} \propto R_j^{-1}$. Thus $B_{\perp}$ decreases slower than $B_{\parallel}$ during the jet expansion and is expected to dominate after some distance from the nucleous.

hot-spots, we can say that the large-scale structures of the extended sources also change character at about the same total power as the major transitions in the jet properties.

(c) *Collimation*: the greater part of the jets in radio galaxies, but only few in QSRs, show lateral expansion. This fact, with the transverse brightness profile that is generally center brightened, supports the interpretation that the synchrotron emission occurs within the jet itself due to some inefficencies in the energy transport, and does not occur in a cocoon around it. Bridle (1984) shows that the resolved jets in powerful sources tend to expand more slowly than those in weak radio galaxies. Thus the narrow one-sided jets dominated by parallel magnetic field tend to feed edge brightened structures with prominent hot spots for the more powerful cases. Whereas the rapidly expandig jets dominated by perpendicular magnetic field tend to feed edge darkened structures without prominent hot spots.

A last note: the changes in the radio jets's properties seem to be related to the core and total radio powers rather than to the optical luminosity of the parent object, (whether the object is a radio galaxy or a quasars). Moreover: the correlations so found cannot by themselves establish one particular model of the energy transport in extragalactic radio sources, or, more in general, in active galactic nuclei. We need to know more about the physics of these jets, their physical parameters, *i.e.* velocity, Mach number, and how these quantities vary with total and core radio power in such a way to produce these correlations. The next paragraph will introduce some parameters of jets and their physical structure.

1.3 Physical Parameters of Astrophysical Jets

It is now a common view of jets as physical conduits along which mass, momentum, energy, and magnetic fields are supplied from the nucleus to the outer components (Begelman, Blandford, and Rees, 1984). From all the data and the variety of jets morphologies, to understand how jets are formed and what keep them collimated over distances, traversing interstellar and intergalactic space, is fundamental. These two issues are equally important, and in this study we deal only with the second one. From the knowledge of jetlike flows in the laboratory, we can infer some properties of astrophysical jets, using gas dynamics and magnetohydrodynamics (MHD).

The first thing to do is to observe the radio emission from these jets. The theory of synchrotron radiation can give a rough estimates of densities, pressures and velocities in single sources. The jet angular FWHM Φ, can be used to characterize how the synchrotron emission widens with angular distance Θ from the radio core. Therefore, at least qualitatively, we can deduce how the flow radius R_j change with the distance z from the core. Moreover, $\Phi(\Theta)$ can reflect the jet magnetic fields $\mathbf{B_j}$ organization, especially on large scales. The expansion rate $d\Phi/d\Theta = 2(dR_j/dz)\sec i$, where i is the angle of the jet to the plane of sky, gives indirect informations on the balance between the jet pressure p_j and the external pressure $p_e(z)$. Freedom or confinement of jets is described from the behaviour of that parameter. In few sources with well resolved jets $d\Phi/d\Theta \to 0$, at projected distances $z \approx 10$ kpc meaning that these jets are not free, even if at VLBI scale (parsec scale) they show collimation. A typical example is the jet in NGC315. It has a local expansion rate of less than 0.09 until $z = 3.5\,\mathrm{kpc}$ from the nucleus, oscillating around the value 0.3 and finally reaching the value 0.09 beyond $100\,\mathrm{kpc}$. This strongly suggest that some confinement mechanism should also act in some region as in the recollimation zone.

Since weak and powerful radio galaxies show different expansion rate, let's summarize the main results in order to have some estimates on the internal and the external pressures.

(a) Weak Radio Galaxies ($P_{tot}^{1.4} < 10^{25}$ W/Hz).

To study the physics of jets propagating in a medium, requires many pieces of informations. Lower limits on p_j are set by the synchrotron properties of the jets. These values range:

$$p_{min} \approx 10^{-10} \text{ dyne/cm}^2 \qquad \text{inner few kiloparsec ,}$$

$$p_{min} \approx 10^{-13} \text{ dyne/cm}^2 \qquad \sim 100 \text{ kpc ;}$$

p_{min} scales with the jet radius R_j roughly as R_j^{-1} to R_j^{-2}. The pressure is minimized when there is almost equipartition between relativistic electron and magnetic energy densities. For example, in the jet associated to the galaxy NGC6251, p_{min} decreases from $\sim 10^{-3}$ dyne/cm^2 within the nucleus,to $\sim 3 \times 10^{-12}$ dyne/cm^2 in the outermost parts, (Perley, Bridle, and Willis, 1984). The corresponding intensity of the magnetic field at equipartition ($B_{eq} \propto (p_{min})^{\frac{1}{7}}$), range from 0.1 G in the compact components to 3×10^{-7} G in the weakest sources. If the jet is thermally confined, p_{min} sets a lower limit to the required quantity $n_e(z)$T. Evidence that the confining agent is thermal pressure of a hot gas comes from X-ray measurements. The minimum X-ray luminosity of an isothermal confining halo between energy E_1 and E_2, is given by:

$$L_X(E_1,E_2) = 1.995 \times 10^{-34} \overline{g}_{E_1,E,} \sqrt{T} \left(exp\left(\frac{-E_1}{kT}\right) - exp\left(\frac{-E_2}{kT}\right)\right) \int n_e^2 dV\, W$$

where $\overline{g}$ is the mean Gaunt factor in the appropriate energy range. The emission measure integral $\int n_e^2 dV$ can be evaluated from $n_e(z)$ with a spherical symmetry assumed for the gas distribution. Under these assumptions, the temperature of the confining gas is ≈ 1 to 3×10^7 K for sources like NGC315, 3C66B, Cen A and NGC6521.

When $d\Theta/d\Phi \ll 1$ for segments of jets and they propagate freely, they are supersonic. Therefore we expect, from the data, that the jets start supersonic, being initially collimated, and become transonic at ≤ 1 kpc from the nuclei. Then they begin to feel the rapid decrease of the external pressure. With $p_e \propto z^{-n}$ and $p_j \propto \rho_j^x$, the sound speed in the jet is given by: $c_s = \sqrt{\Gamma p_j/\rho_j} \propto p_j^{(x-1)/2x}$. The jet is confined when $p_e = p_j \propto z^{-n}$, therefore $c_s \propto z^{(n/2x)-n/2}$. The velocity of expansion is then equal to $v_r = v_j(dR_j/dz) \propto z^{(n/2x)-1}$. To confine a supersonic jet continuosly requires that $v_r > c_s$ if $n > 2$. If p_e scales faster then z^{-2}, the jet free. When the jet encounter a region where p_e scales slower than z^{-2}, (*cf.* the X-ray halo of M87), it can be reconfined. The interface between the jet and the ambient becomes a place where shocks develop, converging toward the jet's axis. The interaction of these shocks can be responsible for the quasi-periodic structures that are often observed in jets, as equally spaced knots and oscillations in the expansion rate (*cf.* NGC35, Willis *et al.* 1981; NGC6251 Bridle and Perley, 1983). Shocks also accelerate relativistic particles (see Drury, 1983; Blandford and Eichler, 1987, for reviews) and reheat the jet (increase the pressure, lower the Mach number; Sanders, 1983).

Bicknell *et al.* (1989), investigated a sample of 23 jets taken from the B2 catalog of low luminosity radio sources studied using the VLA by Fanti *et al.* (1987). In the context of the turbulent jet model of Bicknell (1986), it was found that all 23 jets are initially lighter than the interstellar medium and eventually approach density equilibrium through entrainment of external matter. For most jets the Mach number range from 1 to 3; for few the Mach number could be as high as 10. This study support the notion that the transition from class I to class II radio sources represents mainly the transition from low to high Mach number jets. We will discuss the details of turbulent jets model in chapter 2.

(b) Powerful Radio Galaxies and QSRs ($P_{tot}^{1.4} > 10^{25}$ W/Hz).

The study of Bridle (1984), shows that jets in some powerful sources are:

(*i*) free with mach numbers $M_j \geq 50$,

(*ii*) confined by much larger $p_e(z)$ than that in nearby radio galaxies or

(*iii*) the approaching sides of relativistic twin jets, whose minimum p_j is over-estimated by the conventional calculation due to Doppler boosting since they are all one-sided.

Sources like 3C33.1, 3C111, and 3C219, have jets that do not show a systematic expansion with the increase of the distance from their cores, (see Table 3 in BP). These jets are recollimated at some tens of kiloparsec from the cores, distances greater than those in weaker sources. According to the argument, proposed by Potash and Wardle (1980), there is inconsistency between the free propagation of these jets with the thurst balance. For a nonrelativistic jet the thurst is given by $T_j = \rho_j v_j^2 A_j$ where ρ_j is its density, v_j its velocity and A_j its cross-sectional area. With $v_j^2 = M_j^2 c_s^2$ and $c_s^2 = \Gamma p_j / \rho_j$, we can write

$$T_j = M_j^2 \Gamma p_j A_j \geq M_j^2 \Gamma p_{min} A_j$$

where p_{min} is derived from the synchrotron calculations. From the point (*i*) the estimates on T_j result so large that the jets could not be stopped or bent by the IGM. Therefore M_j or p_j must have been over-estimated.

Begelman and Cioffi (1989) studied the possibility that in powerful radio sources the confinement of the the jet may be due to the cocoon. That is, the cocoon can reach a pressure such to confine the jet if the rate in which the cocoon expands in the IGM is slower than the rate in which the jet delivers its energy. In this case the cocoon is overpressured with respect to the IGM and can confine the jet having the same pressure.

X-ray measurements (temperatures $\approx 1-3\times10^7$ K) require that jets, on the parsec-scale, are Doppler-boosted in several QSRs[5] in order to be thermally confined. That means an over-estimation of p_{min} by a factor $\mathcal{D}^{(8+4\alpha)/7}(\sec i)^{4/7}$ that can result larger than the relativistic correction γ_j^2 to the thurst. This avoid the thurst balance problem if the jet is close enough to the line of sight. On the other hand, the 'Doppler solution' seems not to be always the case. When the jet is thermally confined, the projection required for Doppler boosting increases the *linear scale* of the radio source by $\sec i$; thus the volume of the confining gas increases as $\sec^3 i$. The confinement problem is solved when the increase of the volume filled with confining gas, is balanced by the reduction in n_e^2, that is of p_e. If the beaming cone is wider than $1/\gamma_j$, very small angle to the line of sight are required to solve both the thurst and the confinement problems, but it is difficult to explain the high fraction of jets detected in extended 3CR and QSRs. The X-ray emission detected from clusters of galaxies where radio galaxies with jets are present, is the signature that the cluster gas surrounding the jets is responsible for the external thermal pressure and ram pressure. The estimates for the thermal pressures give values greater than the minimum internal pressures of the jets over several kiloparsec assuring thermal confinement (Burns, *et al.* 1980). This seems to be the case for several large-scale jets associated with low-luminosity radio galaxies, supporting the hypothesis of thermal confinement of those jets.

Magnetic confinement is often invoked for jets in powerful sources, although the data on the expansion rates and the recollimation zones of jets like 3C31, 3C449 and NGC315 are fitted by magnetic confinement as well as thermal confinement. Generally the former mechanism is more efficient than the confinement by external thermal pressure. Gas-pressure confinement cannot cause a significant focusing because the convergence speed of an unmagnetized jet

5 The Doppler factor is given by $\mathcal{D} = \gamma_j^{-1}(1-\beta_j \sin i)^{-1}$.

towards its axis cannot be much greater than the internal sound speed. A more rapid convergence would induce shocks whose dissipation would increase the internal jet entrophy, inhibiting further compression (Norman *et al.* , 1984). Sanders (1983) found numerically that, given for the internal gas pressure an adiabat as $P \propto R^{-2\gamma}$ with $\frac{4}{3} \leq \gamma \leq \frac{5}{3}$, the jet radius will be reduce by a factor of ~ 2. If the jet contains toroidal magnetic field (B_φ in cylindrical coordinates), the speed at which the jet can converge, is comparable to the Alfvén speed $v_A = B_\varphi/\sqrt{4\pi\rho}$ so that a much sharper focusing of the jet can be induced (Achterberg *et al.* 1983). The toroidal magnetic field B_φ is wrapped around the jet and through the pinching mechanism, due to the $\boldsymbol{j} \times \boldsymbol{B}_\varphi$ forces, the self-confinement in the radial direction is ensured. The presence of the azimuthal component B_φ is due to the currents carried inside the jets by the global flow or by surface currents located at the jet boundary. However, a toroidal component of the magnetic field can be generated by helical motions of the flow around the jet axis, stretching the frozen-in magnetic field and giving to it an helical configuration with a toroidal component, (Benford, 1978). There is not yet strong evidence for the existence of toroidal magnetic fields around the jets. They are difficult to detect on the actual radio maps, because they are located mainly in regions of low surface brightness, at the periphery of the jets, since there is lack of relativistic electrons. However, faint emission cocoons are found around brighter jets like M84, 3C341, $1321+313$, and $2354+47$, [BP]. The study of the Faraday rotation[6] and depolarization could provide another evidence of toroidal magnetic fields (Perley *et al.* , 1984).

Estimates on the jets density can be also produced using the calculations from the synchrotron emission since the thermal plasma within the

6 Faraday rotation appears during the propagation of electromagnetic waves in a magnetized plasma. Observation of the effect allow us to derive information on the intensity and direction of the magnetic field, not only in the emitting source region itself, but also in the intervening media.

jet is generally too teneous to be detected directly through emission lines or bremsstrahlung. The Faraday effect rotates the plane of polarization of the synchrotron radiation of an angle $\Delta\varphi \propto \nu^{-2} \int n_e \mathbf{B} \cdot \mathrm{dl}$ where dl is an increment distance along the line of sight. Therefore radiation emitted at different depths within the jets will be rotated of different angles giving as net result the 'depolarization' of the emitted flux. An upper limit on the jet density can be deduce from the rotation measure, $RM = \Delta\varphi/\lambda^2$, when this parameter is not affected by the gas clumped around the source. For example, in sources like 3C31 (Burch, 1979; van Breugel, 1980) and 3C449 (Perley, Willis, and Scott, 1979) a mean value for the number density $n_e \sim 10^{-2}$ cm^{-3} has been found. Faraday rotation measurements, however, do not tell us how the gas is distributed within the jet. It can be localized in clouds and there the magnetic field can be stronger than average, or it can change direction many times along the line of sight. Thus the true density can be different from that estimated from the Farady rotation measurements also because it is difficult to distinguish what is an intrinsic depolarization from what is just a sort of 'screen' effect due to clouds between the jet and the observers.

On the jet velocity determination we will dedicate the next paragraph, since it is crucial to the energy transport in radio sources.

1.4 The Velocity Problem

Observationally we have only one direct measure on the jet velocity: the case of the galactic source SS433, where Doppler-shifted emission lines are observed. They give a value of $v \simeq 0.26$ c, (Margon 1984). There is another case where emission line redshift is detected, (see Coma A; Miley *et al.* 1981), but the relation with the outflow velocity is not well established. Therefore we are forced to relay only on indirect indicators to estimate the jet velocity.

We can list the most common indicators used:

- *Semi-direct indicators*

  Optical emission lines;

- *Indirect indicators*

  Radio morphology;

  Radio brightness distribution;

  Change in angular extent with time;

  X-ray observations;

  Spectral index changes.

We are not going into all the details of these velocity indicators. Instead we are going to discuss their implications in the context of the 'twin-exhaust model' for radio sources, first proposed by Blandford and Rees (1974). Briefly let's summarize what the 'twin-exhaust model' proposes. The model requires a source of relativistic plasma in the nucleus of the parent galaxy or QSO, together with some dynamically unimportant magnetic field. This plasma is extremely hot and inflates a cavity in a surrounding cooler gas cloud. If this cloud is rotationally flattened and axisymmetric, the hot relativistic gas may "break out" in opposite directions along the axis of rotation. If the presumed De Laval nozzle[7] can actually form, the random motion of the relativistic plasma is converted via a sonic transition to cold, collimated relativistic flow.

The main achievement of this model is that it provides the most efficient way of supplying energy to the extended radio sources and that it naturally accounts for their double structure. Moreover, the presence of relativistic motion can explain some phenomena that are observed in the compact radio sources.

---

7 It is known, from fluid mechanics that when we have a one-dimensional flow of gas through a nozzle which first narrows and then widens, the flow reaches a supersonic velocity, (*cf.* Landau and Lifshitz, 1959). Such nozzle is called De Laval nozzle

To discuss the importance of these velocity indicators it is useful to take the following question as guideline: is there relativistic velocity on *any* scale? There are many morphological indicators, especially at large scale (> 10 kpc). For example, when we look for relativistic motion in weak radio sources (FR I, edge-darkened) we face some problems related to the presence of "wisps", "plumes" and "bends" (see the classical example of 3C449; Perley *et al.* , 1979). These morphologies are difficult to associate with a collimated, rather rigid, relativistic flow. On the contrary the outer structures in 3C449 resemble a turbulent, subsonic flow. The surface brightness distribution of these sources has its highest values in the inner regions of the radio structure in the form of bright knots. The 'twin-exhaust model' explains the presence of bright knots at the end of the jets, where jets are decelerated due to the interaction with the medium. That is a place where shocks are generated. This could not be the case for many FR I sources. The common assumption in these sources is that it is possible to produce shocks in the inner regions of the jets without disrupting them; interactions of oblique shocks could do the job. This hypothesis has been tested numerically by Normann *et al.* (1984).[8] Sources like NGC1265 poses similar problems due to the C-shaped morphology.

As we have already mentioned, many radio sources are characterized by an asymmetric structure: jets are detected only on one side of the double structure. We can use this fact as velocity indicator in the following sense: the one sided jet is the result of Doppler enhancement of a weakly emitting jet pointing toward the observer, when the bulk motion away from the nucleus is relativistic on large scale (Doppler boosting). That could be the case for all the

8 They have investigated the behavior of pinching modes in the nonlinear regime. Ordinary mode pinch instabilities, important only at Mach number of the order of unity, are shown to be disruptive. Rotation mode pinch instabilities, important in supersonic jets with parameters of astrophysical interest (*i.e.* low density ratio, high Mach number), are shown to be not disruptive, but rather saturate at finite amplitude through the formation of oblique internal shocks.

one sided jets (Browne, 1983); however this is not a satisfactory explanation of the sidedness problem, infact there are few one sided radio sources whose emission is aligned with the spectroscopically determined rotation axis of the parent galaxy, and this rotation axis lies nearly in the plane of sky. The best example is NGC5128. The study of Wardle (1984) on the largest list of QSRs in a complete sample, has found that all have one sided jets. Statistically one would expect these objects to be lying nearly the plane of the sky; this is the main doubt on the relativistic beaming hypothesis. An other explanation comes from Rudnick and Edgar (1984). They have made the hypothesis of an alternating side at a time ejection from the nucleus itself. In this way one sided jets are natural results but now the major problem is to find a central engine that 'works' in such manner.

1.4.1 Relativistic Motion

Relativistic motion was first proposed to be present in quasars. It was suggested by Hoyle, Burbidge, and Sargent (1966), as a possible solution of what was called the "Compton catastrophe", that occurs when rapid variations in flux density are discovered. With τ the time scale for variations, $c\tau$ is the maximum size that the source can have, since changes cannot propagate faster than the speed of light, c. This can gives an estimate of the photon density in the source and an estimate of magnetic field density. As τ becomes smaller the ratio between the photon density and the magnetic field density increase rapidly; when it exceeds unity the inverse Compton process starts, that is radio or infrared photons of energy $h\nu$ are converted to X-rays of energy $\gamma_e^2 h\nu$ by scattering on electrons with energy $\gamma_e^2 mc^2$, catastrophically quenching the source. The ratio was large but the source appeared stable and the X-rays were weak. Rees (1967) then suggested a relativistic expansion of the source. In this way in the observer's rest frame the surface of the source almost keeps up with the radiation emitted. Therefore the time scale for variations are much

smaller from what a comoving observer would measure, increasing the size of the source.

The best evidence for relativistic motion is certainly the phenomenon of superluminal motion, discovered in 1971 (Cohen *et al.* 1971; Whitney *et al.* 1971): apparent superluminal velocities indicate outflow at a speed close to that of light, apparent transverse velocity of a component, relative to the core, is greater than the velocity of light, and jets in these sources appear one sided on parsec scales, due to Doppler boosting. A narrow relativistic beam, aimed nearly to us, which density decreases outwards and the optical depth is unity near the base, where the base is seen as a very bright spot (the core), is the common model to explain superluminal motion. The kinematics of such beam is discussed in detail by Blandford and Königl (1979). The quasar 3C345 is the best-studied superluminal source (see Biretta, Moore, and Cohen 1986, for a summary of the observations on 3C345 for the year 1979–1984). Other well studied examples are 3C120 and 3C273, all showing a "core-jet" structure at centimeter wavelengths, when observed at scales of one milliarcsecond ($\equiv 1\,\mathrm{mas}$). The core lies at one end of the jet, and there is no counterjet at a level of $50:1$ or more. The jet components have a proper motion, relative to the core, with $v/c > 1$.

As VLBI maps becomes more detailed, new features appear. Jets often show a twisting, bending structure (see Walker, 1984). The question of how to bend a rigid, relativistic beam without disrupting it, arises again because the compact jets are generally assumed to be the base of the flow that powers the entire radio sources. In Kellerman and Pauliny-Toth (1981), other properties of compact sources, which may be used to infer a velocity, are reviewed: time variation of the radio flux, about one half of all compact sources vary at some level – some only by a few percent and some by factors of two or more, and structural changes with time. Doppler boosting is consistent with

the variations detected, although only for about two dozen of sources apparent superluminal motion is well established,[9] even if this is not the only explanation available (see Marscher, A.P., and Broderick, J.J., 1982). The presence of relativistic electrons can provide a source of X-ray emission due to inverse Compton scattering of the radio photons by these electrons. The X-ray flux calculated in some sources (*i.e.* NRAO140)[10] is $100 - 1000$ times the values observed. The transformation between the rapidly moving coordinate systems also explains these weak X-rays observed, since in the moving source the magnetic field is stronger, and the radiation density less than in a stationary source with the same observed spectrum. In practice the argument could be turned around: the X-ray observations can be used to derive a lower limit to the Doppler factor. For $\mathcal{D}$ that varies between 5 and 10 there is a good agreement with the values deduced from the variability and the superluminal motion with those deduced from the X-rays observed.

Everything shows relativistic motion on the small scale, roughly from 1 to 10 parsec, in the context of the actual models, whereas this is not the case for radio sources in rich clusters of galaxies (*i.e.* NGC1265, and 3C465). Here the jets appear 'bent' or 'swept back' by the motion of the galaxy through the intergalactic medium. But one major point remains to be solved: how

---

9 See Zensus, J.A. and Pearson, T.J., 1986, for a recent review on superluminal radio sources and the relativistic beam theory.

10 $0333 + 321$ = NRAO140. Marscher and Broderick (1985) have made VLBI observations of NRAO140 at 1.6, 5.0, and 10,7 GHz. This source has a core and three jet components within 9 mas ($50h^{-1}\csc\theta$ pc), but the spectra of only the core and the first jet component can be estimated with confidence. A synchrotron self-compton calculation for the first jet component based on the homogeneous sphere model, gives a minimum Doppler factor $\mathcal{D}_{min} = 3.7$. This quantity is given in terms of observable quantities by

$$\mathcal{D}_{\rm min} \sim S_{\rm m}\nu_{\rm m}^{-\rm p}\Phi^{\rm p}S_{\rm x}^{-\rm r}(1+{\rm z})^{\rm s}$$

where S_m, ν_m, and Φ are radio quantities: the flux density and frequency at the peak of the synchrotron spectrum and the angular diameter. S_x is the X-ray flux density in a band near 1 keV, and $p \approx 1.3$, $q \approx 1.6$, $r \approx 0.2$, and $s \approx 1.0$, (Marscher 1983; Unwin *et al.* 1983).

do we conciliate this fact with the non-relativistic motion seen on large scale jets ($> 1\,\mathrm{kpc}$)? There has to be a region where the compact jet decelerate at non-relativistic velocities and in this region a good fraction of the entire energy of the radio source is deposited. Is there any possible way to detect this 'deposited' energy? This last point strengthens our leading question that can be re-formulated as follows: is there relativistic motion that is dynamically important on any scale in the radio sources? It needs to be said, at this point, that the scale over which we "need" relativistic motion in the 'all-purpose' model, is set by observational limits only. What seems discriminant, in order to answer to that question, are the Mach number of the jet and the density ratio, η, between the density of the jet and the density of the external medium. Infact we could expect different ways of decelerating, or stopping, a jet according to these two parameters. At the moment numerical simulations of astrophysical jets in different regimes of Mach number and density ratio are the best tool to provide clues, expecially about high powered extended jets where there is no direct evidence for relativistic motion (they are fast but not necessarily relativistic – *i.e.* we may not need $v/c > 0.2$).[11] (Also on the bases of energy considerations, the thrust T_j, the density ρ_j of the jet and the cross-sectional area A_j, it is possible to derive estimates on the jet speeds in the range $v_j \sim 1000 - 10000\,\mathrm{km/s}$, much less than c). These regimes involve supersonic hydrodynamics for high-power sources, and subsonic hydrodynamics for low-power sources. The two offer a behaviour different in several ways that we will discuss in the following paragraph.

---

11 What is important is the bulk kinetic energy of the jet used to accelerate the electrons that radiate through synchrotron emission. Infact, a jet that starts with $v_j \approx c$ from the collimation region, can be decelerated by friction or entrainment to $v_j \ll c$ without losing its kinetic bulk energy (Begelman, 1982). How this deceleration occurs, depends on the Mach number of the jet. If it is high another problem raises: the so called "waste energy" problem (Longair, Ryle and Scheuer, 1973) where the energy powered by the jet is much greater than the energy that the extended components can dissipate as heat or radio luminosity.

1.5 Fluid Model

The first models of astrophysical jets elaborated were purely hydrodynamical in which the magnetic field has no dynamical effects. As mentioned earlier, the 'twin-exhaust model' by Blandford and Rees, is the main example of using fluid dynamical analogies describing jets.[12] Recently Rudnick (1988) found evidences for supersonic fluid flow features in the leading edge of the radio source 3*C*33South. There is no clear interpretation yet if this supersonic fluid flow is the jet itself or a blob structure interacting with the IGM. This is an example of how hydrodynamical considerations determine the appearence and the structure of classical double sources. Also based on modeling of gas flows, Gull and Northover (1973) proposed a model in which the energy is released through bubbles of hot gas along the axis of rotation of the nucleus, rather than 'continuous beams' as in the 'twin-exhaust model'. To some extent an alternative of the continuous outflow from the nucleus, was proposed by Christiansen and Scott (1977), in which they discussed the multiple ejection of dense radio-emitting clouds or 'plasmons' moving through the medium. One major problem is raised by this model: it cannot account for the large-scale dimension of radio galaxies since such a cloud undergoes to adiabatic losses due to the work done by the relativistic particles during the expansion of the cloud. The relativistic electrons have lost great part of their energy and they have to be supplied of *new* energy *in situ* in order to account for the characteristic 'hot-spots' found in many powerful radio sources.

All these models were not concerned with the origin of the jets: jets were assumed, and the models accounted for their global behaviour – propagation, structural and stability properties derived from the solution of the Bernoulli

12 The extent to which the dynamics of an astrophysical plasma can be extrapolated from that found in laboratory fluids is still a matter for debate, (*cf.* Lehay and Williams 1984; Achterberg, Blandford and Goldreich 1983).

equation, not for their microscopical behaviour – *i.e.* the relativistic electrons density and the energy spectrum, fundamental aspects in computing the radio luminosity due to synchrotron emission (see Achatz *et al.* 1990). The starting assumption involves a nearly parallel flow of plasma (relativistic or non relativistic) embedded in a background medium. The flow is isentropic and can be approximated to a one-dimensional fluid for the major part of its length. The presence of magnetic fields motivate the fluid approximation in the description of plasma and generally of dilute gases.[13] Infact when the particles mean free path for Coulomb collision in the jet plasma is large (typically it is larger than the width of the jet), the requirement is that the magnetic field is sufficiently strong so that the particle gyroradius is short compared to the distance over which all the macroscopic quantities change appreciably. The gyroradius for a proton with Lorentz factor γ is $\sim 10^{-12} B^{-1}\,\mathrm{pc}$, and the Debye length for the electrons $(k_e T_e / n_e e^2)^{\frac{1}{2}}$, are both less than the smallest length-scales of the flow patterns, so that charge neutrality is satisfied, unless the particles have energies of $10^9\,\mathrm{eV}$ (*cf.* Lovelace 1976). In this way a group of particles moving at random is converted into a "medium" in which motions are related. However, if the magnetic field has a gradient along the field lines, then the particle motion does not occur along the field lines and the problem is no longer one-dimesional, since the magnetic field has no control on particle motion along the field lines. Aspects concerning the interaction of a jet with an ambient medium were left open by the 'twin-exhaust model' of Blandford and Rees. Yokosawa *et al.* (1982), studied the dynamical interaction of an hypersonic beam with a homogeneous ambient medium. For two regimes of the beam speed (relativistic and non-relativistic) and for different density ratios η, they obtained numerically two types of flow structures: (high η) a ballistic beam with a bow shock at the beam front, and a turbulent beam (low η).

13 A similar fluid approximation is used also in the gas dynamical models of solar winds (Weber and Davis 1967) and supernova remnants.

A further extension of the 'twin-exhaust model' is given by Wiita (1978), in which, keeping the one-dimensional flow approximation, new parameters for the confining gas cloud were derived from the observations (optical, radio and X-ray) and then it was applied to CygnusA as an example with new numerical computations. The existence of a confining cloud of gas for the jet, surrounding the central nucleus, is the key assumption of the 'twin-exhaust model'. Different parameters about its shape, density and temperature could modify the distance from the nucleus where the De Laval nozzle is formed. That is the place where the outflow is collimated, since it is the point that has the minimum cross-section, and becomes supersonic, since the external pressure starts decreasing. The final result is a steady state flow in which the development of Rayleigh-Taylor (R-T) and Kelvin-Helmholtz (K-H) instabilities[14] does not affect the equilibrium (a jet of fluid injected in a stationary fluid –medium– can be entirely disrupted by the K-H instability and the kinetic energy of the jet is converted into turbulent energy). The argument in favor of a steady state flow is based on the time-scales for the R-T and K-H modes to grow. The growth times for the R-T are longer than the dynamical time scale of the flow; instead the K-H modes result in small-scale waves and are rapid enough that the flow can still be treated as steady. Wiita (1978a,b) investigated the effects of these instabilities near the nozzle. Their results are in general accord with the analytical arguments of Blandford and Rees. Because of the extreme difficulty

14 Both involve surface waves. The R-T instability is expected to form when two fluids of different densities are superposed one over the other. If the heavier fluid is on the top of the lighter one, then the interface becomes unstable and the heavier fluid drips down to a lower energy configuration. The same occurs when there is a plasma that is supported by a hotter less dense plasma and/or by a magnetic field. Now the ripples formed on the interface can bend the field lines and the denser plasma flows along them to the troughs where it is further compressed and the less dense plasma rises. A classical analogy for the K-H instability is the generation of water waves by wind over the surface of the water. An example is the case of two incrompressible unmagnetized media separated by an interface with one medium flowing relative to the other (*cf.* Chandrasekhar, 1961).

in obtaining an analytical solution to the equations of gas motion in all but a few simple situations, numerical solutions offer a good way to understand the physics of these jets. As an example let's set up the mathematical description of a relativistic flow and then derive some consequences for the interpretation of astrophysical jets.

1.5.1 Relativistic Flow

We start with the equations of motion for a special-relativistic fluid flow.The energy tensor $T_{\mu\nu}$ for a perfect fluid is

$$T_{\mu\nu} = (\varepsilon + p/c^2)\lambda_\mu\lambda_\nu + (p/c^2)g_{\mu\nu} \tag{1}$$

where ε is the mean density, p is the pressure of the fluid, both in the rest frame of the fluid; λ_μ is the mean four-velocity with $\lambda_\mu\lambda_\nu = -1$.[15] The tensor is symmetric and has ten components which satisfy the four conservation equations

$$\frac{\partial T_{\mu\nu}}{\partial x_\nu} = 0. \tag{2}$$

Thus we have obtained five equations with six unknowns. We need of one more equation, the equation of state for a perfect gas, connecting pressure and density. With m the rest mass of the particle and N its proper number density the equation of state is

$$\varepsilon + p/c^2 = mNG(m\xi), \qquad p/c^2 = N/\xi. \tag{3}$$

The function $G(m\xi)$ has been derived by Synge (1957) for a monoatomic gas; ξ is the reciprocal temperature defined by the absolute temperature Θ through

15 The notation follows Synge (1957); Latin suffixes take the values $1,2,3,4$, and the Greek suffixes the values $1,2,3$, with summation over the appropriate range of values in the case of repeated suffix.

$k\Theta = c^2/\xi$. The second equation in (3) is then the usual gas law $p = Nk\Theta$. The following transformations of the dependent variables $u_\alpha = cG\lambda_\alpha$, $p = c^2N/\xi$, $\rho = mN/G$ are used to obtain the final set of equations of motion that is identical to that one of the non-relativistic case, except that in the equation of state:

$$\frac{\partial(\rho u_r)}{\partial x_r} = 0, \qquad \rho u_r \frac{\partial u_s}{\partial x_r} + \frac{\partial p}{\partial x_s} = 0, \qquad \rho u_r \frac{\partial}{\partial x_r}(h + \tfrac{1}{2}u_r u_r) = 0, \tag{4}$$

where the relativistic enthalpy, h, is defined by $h = \frac{1}{2}c^2G^2$. Even if the relativistic equation of state is more complicated than in the classical gas dynamics, Synge (1957) gave a good semplification of it, for the extreme relativistic limit. He found that the function $G(m\xi)$ can be substituted by

$$mG = 4/\xi. \tag{5}$$

That is, when the temperature of the gas is high enough, the gas behaves like a gas of photons with $p \propto N^{4/3}$. Instead when the effective temperature of the gas is low, the gas behaves 'classically', *i.e.* $p \propto N^{5/3}$. Therefore from a mathematical point of view the systems of equations for a relativistic and non-relativistic gas flow are identical. (What changes is the physical meaning of the independent variables introduced in the transformation). This fact allows us to use the same numerical techniques of classical fluid dynamics. Figures 4-5 report numerical simulations of steady jets (Wilson 1978b; Wilson and Falle 1985). Note the structure and the patterns of the shocks along the length of the jets.[16]

The radio emission in the jet will follow closely the behaviour of the pressure giving rise to the knotty structure observed for the radio brightness. Falle

16 The formation of shocks has been known from laboratory experiments. These experiments use a supersonic jet flowing from a nozzle into a larger receiver containing gas at different pressure. The shock patterns depend on the ratio between the jet pressure and the pressure of the ambient gas. When the jet is axisymmetric, the shock always meets the symmetry axis at right angles, forming a Mach disk.

and Wilson (1985), using the same numerical scheme, found good agreement between the position of the knots in the jet of $M87$ and the position of the shocks in the simulations supporting the view that knots are signatures of shocks occurred during the reconfinement of the jet. On these lines Wilson (1987a) developed a conservative Eulerian hydrodynamical scheme based on the Godunov's method for treating unsteady flows. His jet is a steady supersonic jet, composed of a perfect gas with a polytropic equation of state, $p \propto N^{4/3}$ and the bulk velocity is non-relativistic. With the observations on the shape of jets and the jets boundary he derived the conditions existing in the medium around them. The calculations used as parameters the variations on the Mach number and the variations of the internal and external pressure along the jet in $NGC6251$.

Norman *et al.* (1982), investigated the behavior of a supersonic jet in order to test the 'twin-exhaust model'. Their jet is composed by a non-relativistic gas and contains thermal matter that governs the dynamics. The numerical scheme is an improved version of that one used by Wilson (1978a), with a new second-order monotonic advection and the use of LeBlanc interface for a better treatment of discontinuity between the jet and the IGM gases as a true dynamic fluid boundary. They reproduced the structures, beam, working surface and cocoon, conceived by the Blandford and Rees model. Their results showed that a supersonic jet can propagate efficiently, in the intergalactic medium, with Mach number $M_j \geq 6$. Figure 7 shows typical structures observed in radio

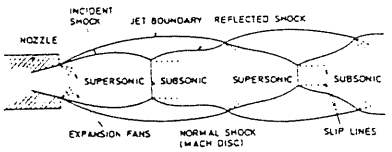

Jet structure behind a highly underexpanded nozzle. Adapted from Adamson and Nicholls (1959).

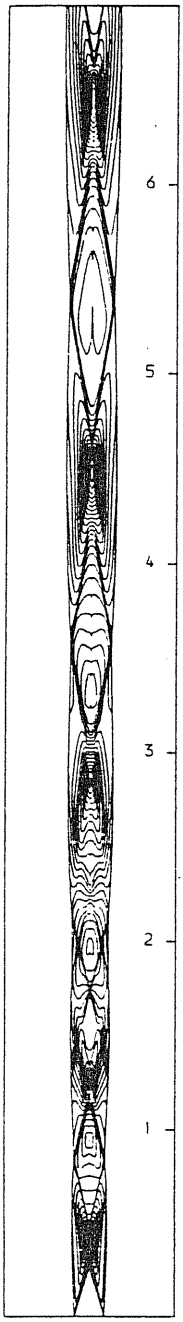

Figure 4: The jet is relativistic and composed by an electron-positron plasma. Forty logarithmic contours of fluid pressure as measured in the rest-frame, for an axisymmetric jet with initial parameters $M_j(0) = 3.5$, $P_j(0) = 1.5$, P_0 and $R_j(0) = 0.08 z_c$, where z is the distance along the jet and z_c is the core radius. The external pressure varies as $P_{ext} = P_0/[1 + (z/z_c)^4]^{1/4}$. The distance scale on the right is in units of z_c. (From Wilson 1987b).

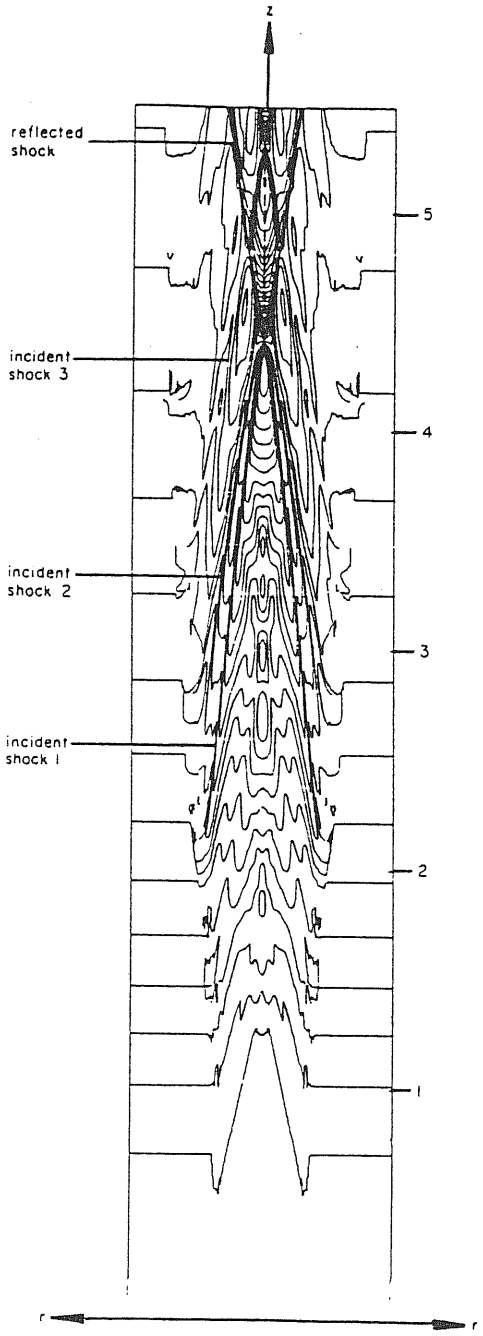

Figure 5: Pressure contours for an axisymmetric steady jet with $M_j(0) = 5$, $P_j(0) = P_0$ and $R_j(0) = 0.2z_c$. The contours are logarithmic with contouring ratio 1.13 : 1, and have been reflected in the symmetry axis. The distance scale on the right is in units of the core radius z_c.(From Wilson and Falle 1985).

jets reproduced by numerical simulations.

Recently Norman *et al.* (1988) showed that a mildly supersonic jet of low luminosity $\leq 10^{25}$ W/Hz can be disrupted when it crosses the discontinuity surface produced by the galactic wind when it encounters the IGM. Such surface represents a standing shock which induces perpendicular internal shocks waves in the jet, which goes from a supersonic regime (Mach 2-5) to a subsonic one, beginning to expand in order to keep up with the pressure of the external medium. They tested numerically the low luminosity jet in CenA, reproducing its global behaviour. This could be the case for others low luminosity jets. The subsonic regime well reproduces a region of the jet where turbulence develops and governs its dynamics.

1.5.2 A Realistic Jet Model

A more realistic jet was investigated by Krautter*et al.* (1983). They considered jets composed of a mixture of protons, electrons and relativistic electrons. The magnetic field has no dynamical effects and it ensures the cohesion of the bulk velocities of the different particles species. The mathematical problem is concerned with a flow in the polar direction and with the angular width (Θ) of the jet, which is an important variable in analyzing the collimation of jets, that needs to be computed by comparison with observation. This model is based on the assumption made by Chan and Henriksen (1980) except on the dynamical importance of the magnetic field. Thus for the flow holds the relativistic equations of conservation of mass and momentum. The internal composition of the jet is treated as a mixture of gases with a adiabat equation of state for each stream line (Synge 1957). A further assumption is that of transverse incompressibility (*i.e.* $p = p(z)$), in which the dynamical variation of the dynamical parameters across the jet are much smaller than those along the jet. This requires that a jet cross section is able to expand in a self-similar

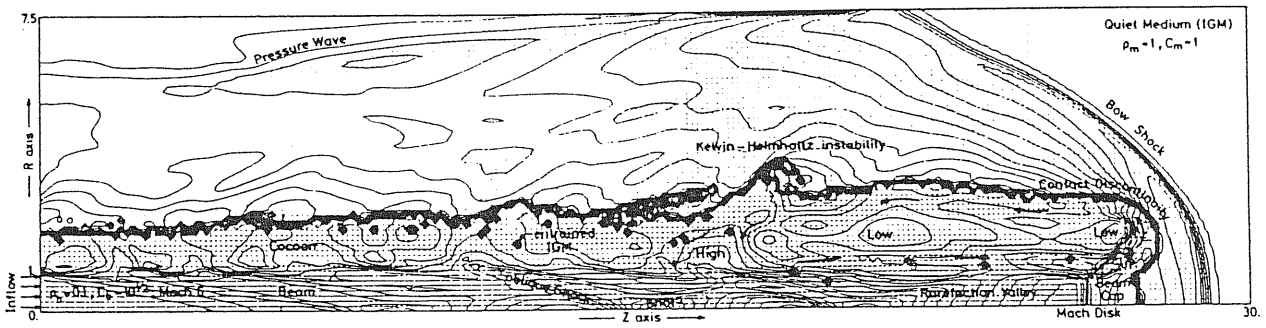

Figure 6: Density contours of a hot ($\rho_b = 0.1$), Mach 6 jet. A beam of gas is injected at the lower left-hand corner with velocity 19; during its propagation it undergoes to deceleration and heating at the Mach disk due to shocks. The working surface moves forward with velocity 4.2, setting up a bow shock in the medium. The cocoon is fed by the high pressure beam cap which first flows laterally and then back along the beam with velocity -7.1 (Mach 1.6). The triple-shock wave configuration generates vorticity which appears as vortical flow in the cocoon. The contact discontinuity is perturbed at the beam cap. These perturbations grow via K-H instability as they advect back along the jet. The cocoon transmits oblique internal shock waves to the beam. At shock reflection high density knots occur. (From Norman *et al.* (1982)).

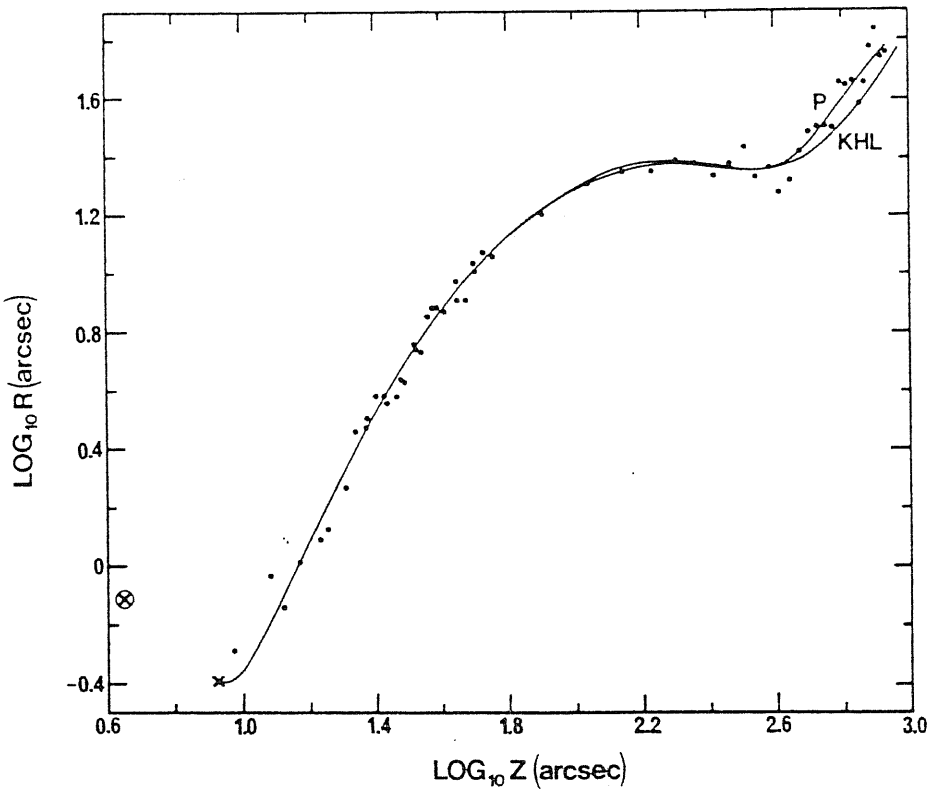

Figure 7: The collimation data for *NGC*315 are fitted by a best polynomial fit, curve labeled P, and by Krautter *et al.* (1983) using the original model of Chan and Henriksen (1980), curve labeled KHL.

or coherently through the action of internal pressure waves propagating transversely. With this analysis of jets they suggested a criteria to distinguish fast jets from slow ones on the bases of their collimation properties. In figure 7 their results are applied to the jet in *NGC*315 compared with those obtained by Bridle *et al.* (1981) applying the original model of Chan and Henriksen (1980).

In all these hydrodynamical models the magnetic field has no dynamical importance on the flow, motivating the fluid approximation for

the plasma. But as soon as magnetic stresses become important for the dynamic of the jet, we have to abandon a gas dynamical description of the flow and use rather a magnetohydrodynamical description. In the next chapter we will introduce such treatment of jets.

2. MHD Model of Jets

2.1 Preliminary Remarks

The presence of magnetic fields in jets is an established fact event if uncertainties on their structure remain. Polarization measurements suggest a sort of regular patterns for the magnetic fields, especially on large scales. They become increasingly important as the source power increases. Lower power sources appear to be thermally confined by an external cluster of gas; the projected field is at right angles to the jet, consistent with an internal helical field, and also with a field which responds passively to the flow and expansion of the source, rather than being dynamically dominant. Higher power sources show overpressure, and may require magnetic self-pinch confinement; the projected field in these sources is along the jet axis, thus requiring the confining azimuthal field to be external to the jet. A theoretical model of jets has to relate these morphological and dynamical correlations (see chap. 1) with the energy flow and especially with some other effects like turbulence and/or shocks which couple the flow energy to the radio luminosity and magnetic and electrodynamic effects. These may be more important in high power sources - *i.e.* jet brightening and confinement (by external azimuthal fields) may occur through current driven turbulence and reconnection effects.

We are going to examine the importance of magnetic fields mainly for the confinement and the stability of jets. Doing that we need to introduce a

description of relevant phenomena such as MHD instabilities and MHD turbulence. We first describe the basic equations of an ideal MHD fluid.

2.2 Basic Equations of Ideal MHD Fluid

Intuitively, an ideal MHD fluid is similar to an ordinary fluid with the important exception that it is highly conducting and magnetized; it is filled with magnetic field lines that exert a force on it. Highly conducting means that the fluid is very strongly coupled with the magnetic field. The field lines are bodily transported by the fluid motion, they are frozen into the fluid, in the sense that currents must always flow in the fluid to make the field conform to the changing densities and directions of the bodily transported lines. In this way the magnetic field is controlled by the fluid motions. On the other hand, the field plays a role in controlling the motion of the field through the tension and the magnetic pressure in the distorted field.

The state of an MHD fluid at any point in space and time is given by the variables $\mathbf{v}$, $\mathbf{B}$, p, ρ, where $\mathbf{v}$ is the macroscopic fluid velocity, $\mathbf{B}$ is the magnetic field, p is the thermal pressure, and ρ is the mass density. The quantities ρ, $\mathbf{v}$ and p satisfy the following equations;[1]

$$\frac{d\rho}{dt} + \rho\nabla \cdot \mathbf{v} = 0, \tag{1}$$

is the equation of mass conservation;

$$\rho\frac{dv}{dt} = -\nabla p + \mathbf{j} \times \mathbf{B} + \mathbf{F}, \tag{2}$$

is the equation of motion. It gives the acceleration of the fluid in response to local forces, $\mathbf{j}$ is the current density, Gaussian cgs units are used with $c = 1$,

1 $d/dt \equiv \frac{\partial}{\partial t} + \mathbf{v} \cdot \nabla$ is the convective derivative which represent the time rate of change at a point that follows the flow of the fluid.

and a force $\mathbf{F}$, which represents the effects of gravity and viscosity. The $\mathbf{j} \times \mathbf{B}$ force can be interpreted as a combination of magnetic tension due to curvature of magnetic field lines - a force directed toward the center of the curvature - and magnetic pressure due to the gradient of the field strength perpendicular to the field - a force directed away from the region of high field strength.

$$\frac{\partial p}{\partial t} = -\mathbf{v} \cdot \nabla p - \Gamma p \nabla \cdot \mathbf{v}, \tag{3}$$

$$\frac{\partial \rho}{\partial t} = -\mathbf{v} \cdot \nabla \rho - \rho \nabla \cdot \mathbf{v}, \tag{4}$$

where Γ is the ratio of the specific heats. These are the thermodynamic equations; the terms $\mathbf{v} \cdot \nabla p$ and $\mathbf{v} \cdot \nabla \rho$ represent the effects of convection. If these terms stood alone, the pressure and density of each fluid element would never change but would simply to be carried along with the fluid. The terms $\Gamma p \nabla \cdot \mathbf{v}$ and $\rho \nabla \cdot \mathbf{v}$ represent the effects of compression and expansion; so pressure and density change as the fluid elements change size in response to change in pressure. The electromagnetic fields satisfy

$$\frac{\partial \mathbf{B}}{\partial t} = -\nabla \times \mathbf{E}, \tag{5}$$

the Farady's law for the evolution of the magnetic field;[2]

$$\nabla \times \mathbf{B} = 4\pi \mathbf{j}, \tag{6}$$

the Ampere's law with the displacement current neglected and

$$\nabla \cdot \mathbf{B} = 0. \tag{7}$$

2 The reason for neglecting two terms the electrostatic force $q\,\mathbf{E}$ in eq. (2) and the displacement current in eq. (6) is that these terms are small compared to others if $B^2/4\pi \ll \rho c^2$ and $(L/T)v \ll c^2$ where L and T are characteristic length and time scales. This magnetostatic approximation is valid whenever the Alfvèn velocity $v_a \equiv B/\sqrt{\mu\rho}$ is much smaller than the speed of light.

When this is the initial condition, Faraday's law ensures that $\nabla \cdot \mathbf{B}$ will be zero for all the time. The Ohm's law couples the fluid and the electromagnetic fields asserting that the current density is proportional to the *total* electric field (in a frame of reference comoving with the fluid), and it may be written

$$\mathrm{j} = \sigma(\mathbf{E} + \mathrm{v} \times \mathbf{B}), \tag{8}$$

where σ is the electric conductivity measured in ohm/cm. We can eliminate $\mathbf{E}$ and j using the Ampere's law, the Faraday's law and with the Ohm's law to give

$$\begin{aligned} \frac{\partial \mathbf{B}}{\partial \mathrm{t}} &= -\nabla \times (\mathrm{v} \times \mathbf{B} + \mathrm{j}/\sigma), \\ &= \nabla \times (\mathrm{v} \times \mathbf{B}) - \nabla \times (\eta \nabla \times \mathbf{B}), \end{aligned} \tag{9}$$

where $\eta = 1/(\mu\sigma)$, is the magnetic diffusivity. After using eq. (7) and the vector identity

$$\nabla \times (\nabla \times \mathbf{B}) = \nabla(\nabla \cdot \mathbf{B}) - (\nabla \cdot \nabla)\mathbf{B},$$

we obtain (for uniform η)

$$\frac{\partial \mathbf{B}}{\partial \mathrm{t}} = \nabla \times (\mathrm{v} \times \mathbf{B}) + \eta \nabla^2 \mathbf{B}, \tag{10}$$

known as induction equation. The magnetic field $\mathbf{B}$ evolves according to the induction equation (10) and the current j needed to produce these currents is determined from eq. (6).The important consequence of this equation is that of freezing the magnetic flux lines into the fluid. It means that magnetic field lines cannot break and change topology in a perfectly conducting fluid. Infact under cosmic conditions the first term on the right-hand side of this equation dominates almost everywhere the second term. Equation (10) then becomes

approximately

$$\frac{\partial \mathbf{B}}{\partial t} = \nabla \times (\mathbf{v} \times \mathbf{B}), \tag{11}$$

while the Ohm's law reduces to

$$\mathbf{E} + \mathbf{v} \times \mathbf{B} = 0. \tag{12}$$

In this large magnetic Reynolds number[3] limit the *frozen-flux theorem* of Alfvén holds: *in a perfectly conducting plasma, magnetic field lines behave as if they move with the plasma.* The exception is in the case of diffusive limit (the magnetic Reynolds number R_m is much less than 1) in which the first term on right-hand side is neglected and the equation of induction becomes a simple diffusion equation for the magnetic field. This implies that field variations on a typical length-scale l_0 are destroyed over a diffusion time-scale $\tau_d = l_0/\eta$.

2.2.1 MHD Instabilities

The importance of MHD instabilities for modeling jets and radio sources, is due to the fact that instabilities generate turbulence that can serve to reaccelerate particles and to amplify the magnetic field. In this case the most relevant MHD instabilities are those of the Kelvin-Helmholtz type. This is a surface instability that occurs in a tangential discontinuity between parallel flows. The interaction between a jet and its confining media is regulated by this instability and its development in space and time. We discuss a simple example of how MHD waves are generated by the K-H instability.

Let's suppose we have an incompressible inviscid flow of two horizontal infinite streams, one above the other, in a gravitational or acceleration field.

3 The magnetic Reynolds number is defined as the ratio of the convective to diffusive terms.

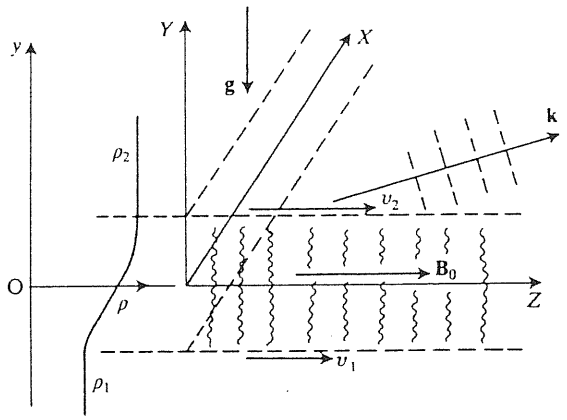

Figure 8: Generation of surface waves.

The interface $y = 0$ is horizontal and the streams on either side of it flow in parallel directions with different velocities and densities. Thus

$$\mathbf{v} = \begin{cases} v_2\,\hat{\mathbf{z}} \\ v_1\,\hat{\mathbf{z}} \end{cases}, \quad \rho = \begin{cases} \rho_2 \\ \rho_1 \end{cases}, \quad p = \begin{cases} p_0 - g\rho_2 y & y > 0, \\ p_0 - g\rho_1 y & y < 0. \end{cases}$$

The two fluids are perfect conductors and are immersed in a uniform horizontal magnetic field $\mathbf{B}_0 = B_0\hat{z}$, fig. 8. We can then use the basic equations of MHD. We look for surface waves propagating along the interface and we assume that perturbations have the form

$$X_1 = \tilde{X}(y)\exp \mathrm{i}(k_x x + k_z z - \omega t), \tag{9}$$

therefore

$$\frac{\partial}{\partial t} \to -\mathrm{i}\,\omega, \qquad \nabla \to (\mathrm{i}\,k_x, \frac{\partial}{\partial y}, \mathrm{i}\,k_z),$$

and

$$\frac{\partial}{\partial t} + \mathbf{v}\cdot\nabla \to -\mathrm{i}\,\omega + \mathrm{i}\,k_z v_0 = -\mathrm{i}(\omega - k_z v_0) = -\mathrm{i}\,\tilde{\omega}, \tag{10}$$

where v_0 is v_2 if $y > 0$, v_1 if $y < 0$ and $\tilde{\omega}$ is the Doppler-shifted frequency.

Taking the derivative respect to y of the MHD equations after linearization they reduce to

$$-\mathrm{i}\left(\tilde{\omega}^2\rho_0 - k_z^2\frac{B_0^2}{\mu} + \rho_0' g\right)\hat{v}_y - \mathrm{i}\,\frac{B_0^2}{\mu}v_y'' + \frac{k_x B_0^2}{\mu}v_x' + \tilde{\omega}\hat{p}' = 0, \tag{11}$$

$$-\mathrm{i}\,k_x\frac{B_0^2}{\mu}\hat{v}_y' - \left(\tilde{\omega}^2\rho_0 - \frac{k^2 B_0^2}{\mu}\right)\hat{v}_x + k_x\tilde{\omega}\hat{p} = 0, \tag{12}$$

$$-\mathrm{i}\,\tilde{\omega}^2\rho_0\hat{v}_y' + k_x\tilde{\omega}^2\rho_0\hat{v}_x + k_z^2\tilde{\omega}\hat{p} = 0, \tag{13}$$

where $k^2 = k_x^2 + k_z^2$. We choose solutions of eq.s $(11-13)$ that decay exponentially as $y \to \pm\infty$:

$$\hat{v}_y = \hat{v}_y(0)\exp(\mp k_y y), \tag{14}$$

where the minus sign holds for $y > 0$, and the plus sign for $y < 0$, and k_y is a positive number whose value is given by the a non zero solution of eq.s $(11-13)$ at a sufficiently large distance from the interface for the density gradient to be negligible, which reduces to

$$(k_y^2 - k^2)\left(k_\parallel^2\frac{B_0^2}{\mu} - \tilde{\omega}^2\rho_0\right)^2 = 0. \tag{15}$$

The final relation is the dispersion relation for these surface waves

$$\rho_1(\omega - k_\parallel v_1)^2 + \rho_2(\omega - k_\parallel v_2)^2 = gk(\rho_1 - \rho_2) + 2k_\parallel^2\frac{B_0^2}{\mu}. \tag{16}$$

In the case of no velocity discontinuity, eq. (16) reduces to[4]

$$\omega^2 = gk\frac{\rho_1 - \rho_2}{\rho_1 + \rho_2} + \frac{2k_\parallel^2 B_0^2}{\mu(\rho_1 + \rho_2)}. \tag{17}$$

It is interesting to study the case in which a given mode is suppressed. This

4 Note that the classical Rayleigh-Taylor instability is recovered since $\omega^2 < 0$ when $B_0 = 0$, or $k_\parallel = 0$, and $\rho_2 > \rho_1$.

occurs when for the magnetic field holds

$$B_0^2 > \frac{\mu g k}{2k_\parallel^2}(\rho_2 - \rho_1), \tag{18}$$

that is short wavelengths are stabilized, whereas sufficienlty long waves are not. Long waves are always unstable when the acceleration is directed from the heavier to the lighter fluid.

Let's define the following quantities:

$$\omega_0^2 \equiv gk\frac{\rho_1 - \rho_2}{\rho_1 + \rho_2}, \quad v_a^2 \equiv \frac{B_0^2}{\frac{1}{2}\mu(\rho_1 + \rho_2)}, \quad \tau_a \equiv \frac{1}{k_\parallel v_a}, \tag{19}$$

ω_0 is the growth rate of the instability in the absence of the magnetic field, v_a is the speed of propagation of an Alfvén wave along the interface and τ_a is the time it takes for an MHD wave to move a distance $v_a\tau_a$. The stability condition from eq. (17), *i.e.* $\omega^2 > 0$, can be expressed as $\omega_0\tau_a \leq 1$. This is a condition on the growth rate of the MHD wave. Infact the stability is reached when the wave propagating along the interface is short enough to connect regions where the fluid is falling to region where the fluid is rising. The roots of the dispersion relation can be written as

$$\omega = k_\parallel \frac{\rho_1 v_1 + \rho_2 v_2}{\rho_1 + \rho_2} \pm k_\parallel \left\{ -\frac{\rho_1\rho_2}{(\rho_1 + \rho_2)^2}(v_1 - v_2)^2 - \frac{\omega_0^2}{k_\parallel^2} + v_a^2 \right\}^{\frac{1}{2}}. \tag{20}$$

It is easy to see that when $\omega_0 = 0$, *i.e.* no acceleration field, the instability condition for the flow becomes:

$$|v_1 - v_2| > \frac{\rho_1 + \rho_2}{(\rho_1\rho_2)}^{\frac{1}{2}} v_a = \sqrt{2}\left(\frac{B_0^2}{\mu\rho_1} + \frac{B_0^2}{\mu\rho_2}\right)^{\frac{1}{2}}. \tag{21}$$

Even if the magnetic field is absent the instability is ensured by the velocity discontinuity.

2.2.2 MHD Turbulence

In fluid mechanics a turbulent flow is a flow characterized by the presence of an extreme disorder of the velocity in time and space. By its nature a turbulent flow is unstable: a small perturbation, due to nonlinearities in the equations of motion, will result amplified. In a viscous fluid flow, which is initially irrotational (with zero vorticity - *i.e.* $\omega = \nabla \times \mathrm{v} = 0$), vorticity is generated at its boundary. This vorticity diffuses throughout the flow which will become fully turbulent (*cf.* Van Dyke 1982).

The scenario is more complicated when the fluid is a plasma, as in jets, radio sources and generally in astrophysics. A plasma is a system defined by a large number of degrees of freedom; this implies that when in the plasma intense waves are present whose mode is in a narrow frequency range, the interaction between these waves will redistribute the energy over all possible modes and frequencies (*cf.* Kaplan and Tsytovich 1973). These interactions play the same role played by collisions in an ordinary gas.

The state of turbulence in a plasma is characterized by the existence of excited waves in a wide range of frequencies and of wavenumbers. MHD turbulence are low-frequency waves (particularly shock waves) with frequencies much less than the average collision frequency, whose wavelengths (motions) are comparable to the dimensions of the hole system governing the structure, form, energy content, and motion of an astrophysical object. Short-wavelength waves, generally defined as plasma turbulence, are relevant for the most powerful electromagnetic radiation of the plasma and the acceleration by the plasma particles to ultra-relativistic energies.[5]

In radio sources the fluctuations in the total and polarized intensity are signature of turbulence. The regions where the total intensity or the magnetic

5 It is the long wavelengths or MHD turbulence that can be resolved observationally.

field is higher are due to compressible (subsonic) turbulence in which the field strength as well the field direction fluctuates. The interpretation of these fluctuations observed depends on what is our model for their sources. There are different ideas on that. The first and perhaps the most likely is that fluctuations reflect turbulence of the synchrotron emission. Instead De Young (1980), together with the kinetic and magnetic energy required the presence of other two quantities which may have nonzero averages: kinetic and magnetic helicities, $\boldsymbol{v} \cdot \nabla \times \boldsymbol{v}$, and $\boldsymbol{b} \cdot \nabla \times \boldsymbol{b}$. In his analysis helicities are the key parameters to produce magnetic energy in radio sources. Helicity turbulence, given the maximum value for the kinetic helicity, can produce magnetic fields of the order of microgauss that can grow in the typical time scale for radio sources of 10^8years on large scales ($> 10\,\mathrm{kpc}$). How is such helicity generated? It can be due to the interaction of the jet with the surrounding ambient especially in the hot-spots region.

There are many approaches to describe MHD turbulence, and the heart of each is constituted by a study of the dynamical or time evolution of the energy (kinetic and magnetic) spectra. The standard approach in turbulence[6] theory is characterized by the following parameters: the total turbulent power, the energy spectrum, characteristic length scales, degree of anisotropy, and degree of compressiveness.

As example we discuss turbulent fluctuations present in radio sources (Eilek, 1989) where the power spectrum is the Fourier transform of the autocorrelation function. The analysis is identical to that for incompressible fluid turbulence. In particular we will examine the magnetic field fluctuations since they are important to radiation. These fluctuations are decomposed into a randomly fluctuating velocity and magnetic fields, ($\mathbf{B_r}$), superposed to an

6 From hereafter for simplicity 'turbulence' stands for MHD turbulence.

uniform magnetic field $\mathbf{B_0}$ different from zero

$$\mathbf{B} = \mathbf{B_0} + \mathbf{B_r}. \tag{22}$$

In turbulence theory the important quantity is the energy density in the random component, $E^B = \langle B_r^2 \rangle / 8\pi$, where the brackets indicate slowly-varying means, describing an ensemble average over all of the turbulent source.[7] In the analysis of propagation of random fluctuations, the distribution of energy as a function of the wave number $k = 2\pi/\lambda$ requires the introduction of the following quantity: the double-correlation functions or covariances of the field variables, which represent a second-rank tensor depending on two points in space and time. The Fourier decomposition of this function of the ith and jth components of the random field $\mathbf{B}$ has the form

$$C_{ij}^B(\mathrm{r}) = \langle B_{ri}(\mathrm{x}) B_{rj}(\mathrm{x}+\mathrm{r}) \rangle, \tag{23}$$

where the brackets indicate the average over all the position vectors x within the source. An immediate result is that the total energy density in the random field is proportional to $C_{11}^B(0) + C_{22}^B(0) + C_{33}^B(0)$. The Fourier transform of eq. (23), is the power-spectrum tensor

$$C_{ij}^B(\mathrm{r}) = \int \Phi_{ij}^B(\mathrm{k}) e^{i\,\mathrm{k}\cdot\mathrm{r}} d\,\mathrm{k}. \tag{24}$$

Continuing this spectral analysis, expressing the ith component of the random field as a Fourier integral and relating the power-spectrum tensor to the complex transform of the ith component of the random field we end up with the

7 In a statistical description of the flow, an ensemble average for a field described by a random function defined on a sample space, represents a statistical average performed on an infinite number of realizations (see *e.g.* Lesieur 1987).

following expression for the magnetic energy density:

$$\langle B_{\rm r}^2 \rangle = \int \Phi^B({\rm k}) d\,{\rm k}. \tag{25}$$

In this way $\Phi^B(\mathrm{k})$ measures the magnetic energy density in the magnetic field at a wave number k and has units $\mathrm{G}^2\,\mathrm{cm}^3 = \mathrm{ergs}$. Numerical and analytical methods give the following results for the magnetic field spectrum : for three-dimensional turbulence, $\Phi^B(\mathrm{k}) \propto \mathrm{k}^3$ for large scales in helical turbulence and $\Phi^B(\mathrm{k}) \propto \mathrm{k}^{-7/2}$ for small scales (*e.g.* De Young 1980). For two-dimensional turbulence $\Phi^B(\mathrm{k}) \propto \mathrm{k}^{-7/3}$ for large scales and $\Phi^B(\mathrm{k}) \propto \mathrm{k}^{-11/3}$ for small scales (Fyfe, Joyce, and Montgomery 1977).

Note that if the turbulent field is symmetric or isotropic eq. (25) can be further simplified to give the generally known turbulent spectra. The final expression is

$$\langle B_{\rm r}^2 \rangle = \int E^B(k) dk, \tag{26}$$

where $E^B(k)$ is the energy spectrum and is interpreted as the energy at k in the random magnetic field. It is defined as $\Phi^B(\mathrm{k})$ integrated over all allowed directions of k. Therefore we have $E^B(k) \propto k\Phi^B(k)$ in the case of two-dimensional (anisotropic) turbulence, and $E^B(k) \propto k^2\Phi^B(k)$ for isotropic turbulence.

There are some characteristic length scales that can be defined for a turbulent flow.

a. Correlation length: the scale above which $C^B(\mathrm{r})$ goes to zero.

b. Driving scale: the scale on which energy is added to the turbulence.

c. Dissipation scale: the scale on which viscous or resistivity processes damp the turbulence. Typically it is a small-scale effect unresolvable in radio sources.

2.3 Stability of Jets: the Role of the Magnetic Field

Jets are affected by many kind of instabilities. These depend on the model used to describe the jet and on the regions where stability is studied. Of course the existence of jets is guaranteed when: (a) the growth rates in space and time of instabilities are slow enough that the jet is not disrupted in a time shorter than its lifetime or in a distance shorter than its length, and (b) damping mechanisms occur and dissipate unstable modes.

As explained earlier in 2.2.1 the most important instabilities for jets are small perturbations of the Kelvin-Helmholtz type. Those instabilities determine the interaction between the jet and its surrounding ambient via mass and momentum exchange. This interaction is typically a non-linear phenomena and numerical and analytical studies give both interesting results. The analytical approach usually begins studying the linearized continuity and momentum equations which then give the dominant modes of instabilities. This has been done for subsonic, supersonic, relativistic, thermally and magnetically confined jets where they have been always assumed as cylindrical beams.[8]

Let's now consider in detail the stability of a magnetized jet (Cohn 1983). The physical model of the jet does not differ from what we have discuss so far, that is: (1) the azimuthal and longitudinal components of the magnetic field scale with the jet radius according to $B_\phi \propto R^{-1}$ and $B_z \propto R^{-2}$ respectively, (2) for the interior of the jet an adiabat equation of state holds and the internal pressure varies with the radius as $p \propto R^{-2\Gamma}$. As a further simplification let us assume that there is an external azimuthal magnetic field and that the velocity

8 See *e.g.* Ferrari, A., Trussoni, E., and L. Zaninetti (1981); Cohn, H. (1983); Fielder, R., and T.W. Jones (1984); Ferrari, A., Trussoni, E., and L. Zaninetti (1978); Turland, B.D., and P.A.G. Scheuer (1976); Blandford, R.D., and J.E. Pringle (1976).

profile and the pressure profile have a top-hat[9] form with a discontinuity at the jet boundary. The state of equilibrium is then characterized by

$$v_z = \begin{cases} u & (r < R) \\ 0 & (r \geq R) \end{cases}, \tag{27}$$

$$v_r = v_\phi = 0\,, \tag{28}$$

$$\rho = \begin{cases} \rho_i & (r < R) \\ \rho_e & (r \geq R) \end{cases}, \tag{29}$$

$$p = \begin{cases} \frac{B_0^2}{8\pi} & (r < R) \\ 0 & (r \geq R) \end{cases}, \tag{30}$$

$$B_\phi = \begin{cases} 0 & (r \geq R) \\ B_0(R/r) & (r \geq R) \end{cases}, \tag{31}$$

$$B_r = B_z = 0. \tag{32}$$

As in standard linear theory stability analysis we choose perturbations for the density, pressure, current and magnetic field, ρ_1, p_1, and $\boldsymbol{B}_1$), of the form

$$\xi(r) = \xi(r) \exp\left(ikz + i\ell\phi - i\omega t\right), \tag{33}$$

where z, ϕ, t are the coordinates used in the Fourier expansion of the perturbation since the equilibrium state is independent of them. Eq. (33) describes Fourier modes with mode number $\ell = 0, \pm 1, \pm 2, etc.$, which represents pinching, helical twisting and fluting modes *etc.* . Linearizing the continuity and the momentum equation of an ideal MHD fluid in those coordinates, we end

9 The top-hat assumption in the velocity profile presumes that the jet boundary has no thickness. This seems to be not the case and this assumption is reasonable when the thickness of this layer is much smaller than the jet width. Numerical simulation showed that (Norman *et al.* 1982). A finite-thickness layer can effect modes due to K-H instability. Ferrari *et al.* (1982) discussed the importance of this phenomena in the context of jet stability.

up with the dispersion relation relating frequency ω and the wavenumber k for each Fourier mode ℓ. In our case we have two physical regions, internal and external at the jet where we find the following modes:

$$\frac{d^2 p_1}{dr^2} + \frac{1}{r}\frac{dp_1}{dr} - \left[k^2 - \frac{\omega_d^2}{c_s^2} + \frac{\ell^2}{r^2}\right] p_1 = 0\,, \tag{34}$$

which is the interior mode (where $\omega_d \equiv \omega - ku$ is the Doppler-shifted frequency), and the exterior mode is

$$\varepsilon_{\rm A}\frac{d}{dr}\left[\frac{R^2}{\varepsilon_{\rm A} r^2}\frac{1}{r}\frac{d}{dr}(rB_{1\phi})\right] + \varepsilon_{\rm F}\frac{\omega^2}{v_{\rm A0}^2}B_{1\phi} = 0, \tag{35}$$

$$\varepsilon_{\rm A} \equiv 1 - \frac{v_{\rm A0}^2}{\omega^2}\frac{\ell^2}{r^2}\frac{R^2}{r^2}, \quad \varepsilon_{\rm F} \equiv 1 - \frac{v_{\rm A0}^2}{\omega^2}\left[k^2 + \frac{\ell^2}{r^2}\right]\frac{R^2}{r^2}; \tag{36}$$

$v_{\rm A0}^2$ is the Alfvèn velocity at the jet radius, $\varepsilon_{\rm A}$ and $\varepsilon_{\rm F}$ are the Alfvèn and the fast mode functions. The interior mode is purely acoustic since the magnetic field inside the jet vanishes. Instead the exterior mode is purely magnetic since the gas pressure vanishes outside the jet. In this way all perturbation variables can be expressed in terms of p_1 and $B_{1\phi}$ in the respective zones. In order to solve eq.s (34) and (35) we have to consider the boundary condition for p_1 at $r = 0$, and $B_{1\phi}$ has to vanish for $r \to \infty$ since there must be no energy radiated inward from infinity. Then

$$\frac{\rho_i \omega_d^2 p_{1-}}{\rho_e (dp_1/dr)_-} + \frac{v_{\rm AO}^2}{R} = \varepsilon_{\rm A+}\omega^2 \frac{RB_{1\phi+}}{d(rB_{1\phi})_+/dr} \tag{37}$$

is the boundary condition needed where the subscript minus (−) and plus (+), indicate the direction from which r approaches to R. The solutions of eq.s (34) and (35) together with eq. (37) represent the dispersion relation for normal modes of a magnetically confined jet.[10] Unfortunately the only analytic solution exists for pinching modes ($\ell = 0$) since eq. (35) has three regular singular points and an irregular singularity at infinity.

10 The fact that their waves fronts are normal to the flow direction implies in principle the maximum rate of momentum transfer from the jet to the ambient.

The final dispersion relation for pinching modes is given as function of the confluent hypergeometric function $y(\omega, k, r)$ (Cohn 1983). It can be written as

$$\rho_i \omega_d^2 \frac{I_o(\kappa R)}{\kappa R I_1(\kappa R)} + \rho_e = \rho_e \frac{R^{-1}\omega^2}{[d\ln y/dr]_{r=R}} \tag{38}$$

where $\kappa = k^2 - \omega_d^2/c_s^2$, and I_0 and I_1 are the modified Bessel functions of the first type.

Through the marginal stability analysis of the dispersion relation so found (*i.e.* for those values of ω, k, where $\mathrm{Im}(\omega) = \mathrm{Im}(k) = 0$, but in the vicinity of which these imaginary parts are different from zero), Cohn (1983) showed that the pinch instabilities change character depending on the Mach number M of the jet and the density ratio η. This result was confermed by Norman *et al.* (1984) and it is reported in figure 9. The structure of the pinch modes changes according to the number of internal nodes present in the radial function of the perturbation variables (*i.e.* the function $y(\omega, k, r)$).

An ordinary mode (OM) or fundamental mode has no internal nodes, whereas the reflection modes (RM)[11] constitute a family parametrized by the number of internal nodes. The RM modes are repeatedly reflected near the shear surface and the non linear amplitude grows. Due to this mechanism the RM modes possess also a transverse component while the OM modes are purely longitudinal. Numerical simulation by Payne and Cohn (1985) are shown in figure 10. They studied the importance of the reflection modes for the jet stability. It is interesting to see the change of their character from longitudinal to transverse of OM and RM modes.

Subsonic jets result unstable to a single mode (OM) at every wavenumber. For supersonic jets the confinement is due to ordinary and reflection modes.

11 A RM modes is characteristic of supersonic shear surfaces. A plane linear wave will be reflected with a greater amplitude for certain angles of incidence.

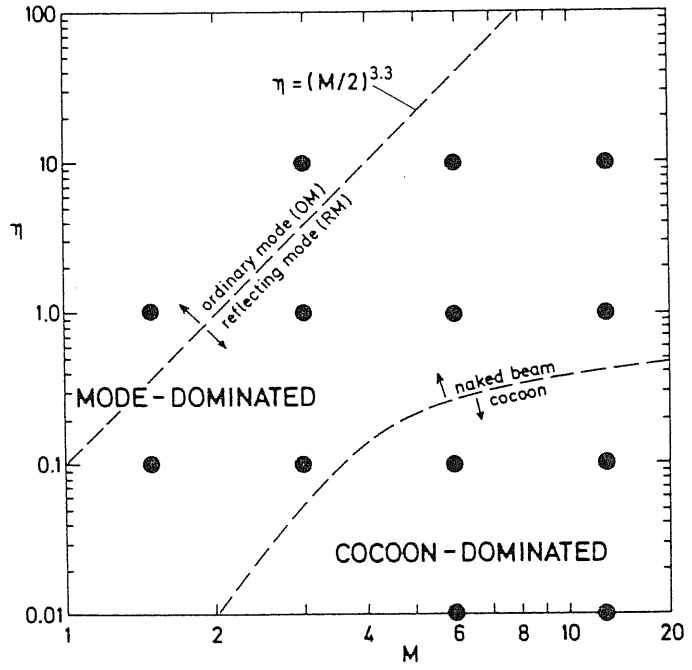

Figure 9: The parameter space (M, η). Boundary between ordinary mode reflection mode, and cocoon dominated regions are shown (dashed lines). Black dots are the 13 cases studied numerically by Norman *et al.* (1984) and by Cohn (1983). Of the 13 cases studied only 7 satisfying $M > 2\eta^{0.3}$ are interesting. The jets with parameters lying below the lower dashed line exhibit shock structures driven by perturbation in the surrounding cocoon. The seven jets remaining have essentially no cocoons ("naked beams").

RM modes result to have large spatial growth rates such that they may be responsible for the observed knots in jets. In the parameter space M, η the change between the region dominated by OM modes from the region domi-

nated by RM modes, occur for $\eta \geq (M/2)^{3.3}$. Jets satisfying $M < 2\eta^{0.3}$ lie in the OM mode dominated regime and interact with the ambient mainly through mass exchange in a mixing layer at the jet boundary. Jets satisfying $M > 2\eta^{0.3}$ lie in the RM mode dominated region. The interaction occurs mainly through shocks. There is only momentum exchange and no mass exchange. In other word we can say that RM dominated jets are a more efficient mechanism to transport energy since they are only subject to some internal dissipation of kinetic energy due to the presence of shock waves. On the contrary the OM dominated jets are subject to deceleration and disruption since they substantially entrain matter from the surrounding medium. Such behaviour can in principle explain the morphological classification of extended radio sources by Fanaroff and Ryle (1974). That is lower power sources will have jets in the OM dominated regime, and high power sources will have jets in the RM dominated regime.

An interesting comparison between magnetized and unmagnetized jets has been carried out by Lind *et al.* (1989). They examined numerical simulations of light ($\eta = \rho_j/\rho_e \leq 0.1$) hypersonic jets, including the effect of a toroidal magnetic field. The jet is injected into a uninform and possibly magnetized ambient medium. Their results for unmagnetized jets are in line with those discussed precedently (*cf.* Norman *et al.* (1982); Wilson and Falle (1985); Payne and Cohn (1985)). The jet material ignores the small Mach disk formed and is deflected by weak oblique shocks and then decelerated to subsonic speed at a strong anular shock formed near the contact discontinuity between the shocked jet fluid and the shockedambient gas (figure 11). After passing the anular shock, most of the matter expands and enters the backflow. Some material enters the 'plug' ahead of the Mach disk. The gas accumulated in the plug is discharged intermittently by the shedding of vortices. These votrices in the cocoon generate secondary shocks, since the subsonic backflow can expand adiabatically thus becoming

locally supersonic. The interaction of these secondary shocks with the beam produces strong pinchies that could be interpreted as a localized enhanced confinement (*cf.* Norman *et al.* (1982)).

The case of a magnetized jets, add new information on the confinement mechanisms and more generally on the jet structure. The main differencies can be stated as follows:

- a magnetized jet advance in the medium faster than an unmagnetized jet in the same conditions of thurst and ambient;
- for the magnetized jet the flow beacomes transonic closer to the origin than in the unmagnetized jet.

The main reason for this last point, is that the presence of a toroidal magnetic field changes the shock structure. Infact the shocked gas does not flow in the cocoon but is refocused toward the jet axis by the toroidal field and then it flows into the plug. This plug represents a sort of magnetic trap for the shocked gas that lengthens with time. When the gas pressure overcomes the magnetic pressure in the plug, the gas material is discharged in the cocoon and the cycle restarts. In other words in a magnetized jet the forward-moving plug has the same function of the backflowing cocoon, giving to the jet a more streamlined shape preceded by stronger shocks. Observationally these are features that can be distinguishable – *i.e.* the jet in *NGC*1068 shows strong bow shocks and a streamline shape (Wilson and Ulvestad (1987)). These numerical simulations are the first attempt to include a dynamically important toroidal magnetic field. They can be improved especially including the treatment of relativistic magnetized jets, since we know that relativistic velocities are present in jets.

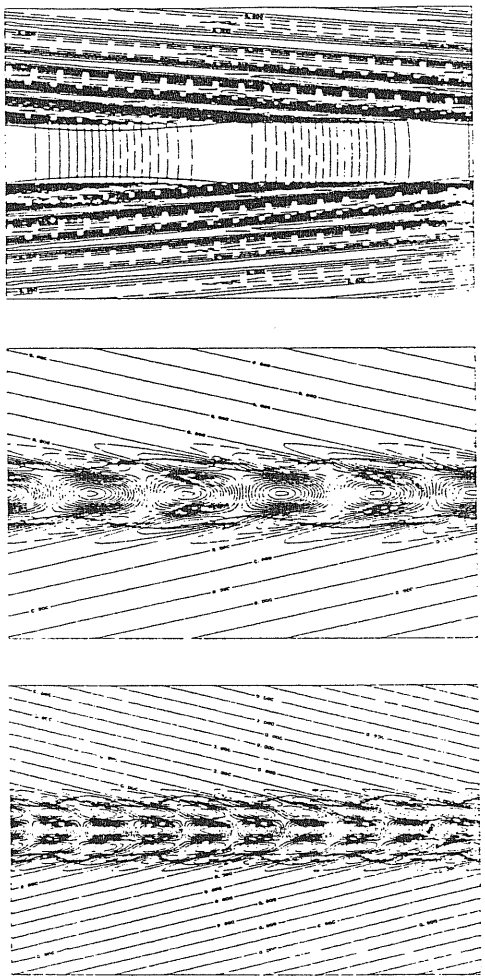

Figure 10: Contour plots of the pressure perturbation inside and outside the jet, for the pinching mode ($\ell = 0$) for $M = 5$ and $\eta = 0.1$ out to a transverse extent of $5R$ and over a longitudinal extent of $16R$. Solid lines correspond to regions which are overpressured, dashed lines to regions underpressured. (Top) Pressure perturbation for the fundamental mode ($n = 0$). The internal structure of the mode is purely longitudinal. (Middle) Pressure perturbation for the first Rm mode ($n = 1$). The transverse character of the RM mode is visible. The interior part of the jet is filled by knotlike features. (Bottom) Pressure perturbation for the second RM mode ($n = 2$). The transverse structure becomes more complicated.

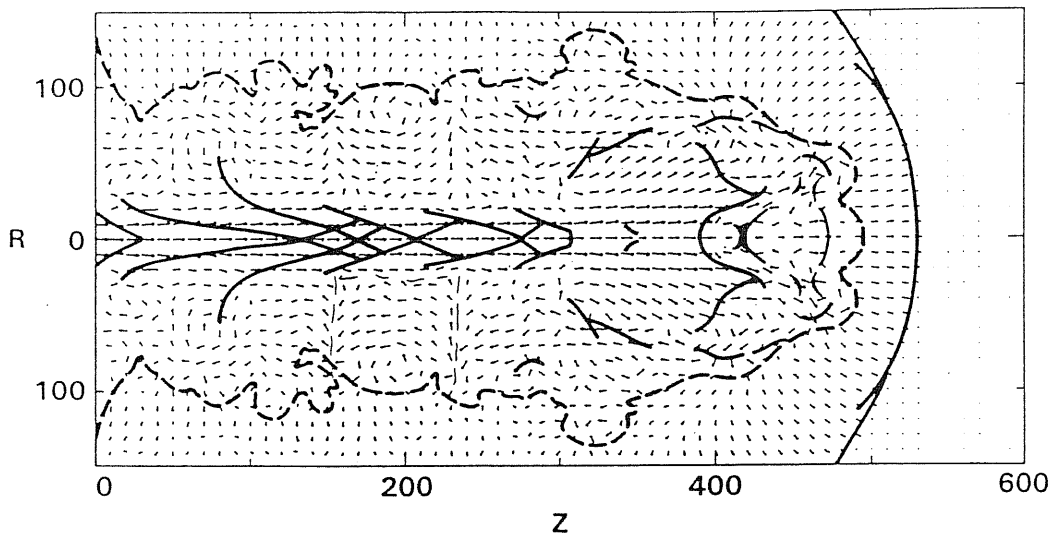

Figure 11: Position of shock waves (solid lines) and contact discontinuity (dashed lines) superposed on velocity vectors foe a jet with $\eta = 0.1$ and $M = 6.1$. The lengths of the velocity vectors are linearly proportional to the magnitude of the velocity. Much of the matter is deflected from its flow in the "beam" by an oblique shock out towards the anular shock where most of the deceleration takes place (from Lind *et al.* (1989)).

2.4 Turbulent Jets

Turbulent phenomena in radio sources usually arise from Kelvin-Helmholtz instability at the interface between the jet and the surrounding medium. This instability may disrupt the jet, and relativistic effects have been studied in order to suppress it (Turland and Scheuer 1976; Blandford and Pringle 1978). We have already shown as this instability occurs in a shear layer of finite thickness (*cf.* Norman *et al.* 1982). This is the mixing region where turbulent motion characterized by large-scale shear rises. Low Mach number jets seem to be more affected by this fact since in high Mach number jets unstable

modes have lower growth rates. Observations of low luminosity radio sources can be interpreted according to this view. Infact they show jets that expand typically of a cone angle of about $15° - 20°$ together with a slow decrease in their surface brightness.[12] The most reliable observational evidence of turbulent motion is given by the effects of turbulence in the synchrotron emission. In particular fluctuations of the magnetic fields in intensity and in direction would influence the total intensity emitted and its polarization. The study of polarization in determining the turbulence structure has been investigated by Laing (1981): he examined the correlation between the polarization of a source and the amplitude of an isotropic turbulence. Fanti *et al.* (1982) interpreted the slow decrease in brightness in those jets with some adiabat processes associated with entrainment. Their results for the surface brightness of an adiabat jet are:

$$f(p) \propto (v_{jet}R^2)^{-s/3}p^{-s}$$

is the electron distribution function; R is the jet radius and s is the spectral index;

$$\boldsymbol{B}_{\parallel} \propto R^{-2}, \quad \boldsymbol{B}_{\perp} \propto (v_{jet}R)^{-1}$$

are the magnetic field components and finally the surfaces brightness derived is

$$I_{\nu} \propto v_{jet}^{-s/3}R^{1-2s/3}B^{(s-1)/2}.$$

Based on those interpretations Bicknell (1986a,b) proposed an argument according which jets in edge darkened (FR I class) sources are essentially low Mach number for almost their entire length, they are non-dissipative and their morphology and surface brightness is governed by turbulent processes. His

12 Their decrease in the surface brightness is not compatible with the decrease expected for a constant-velocity laminar jet since its deceleration is much slower than that observed.

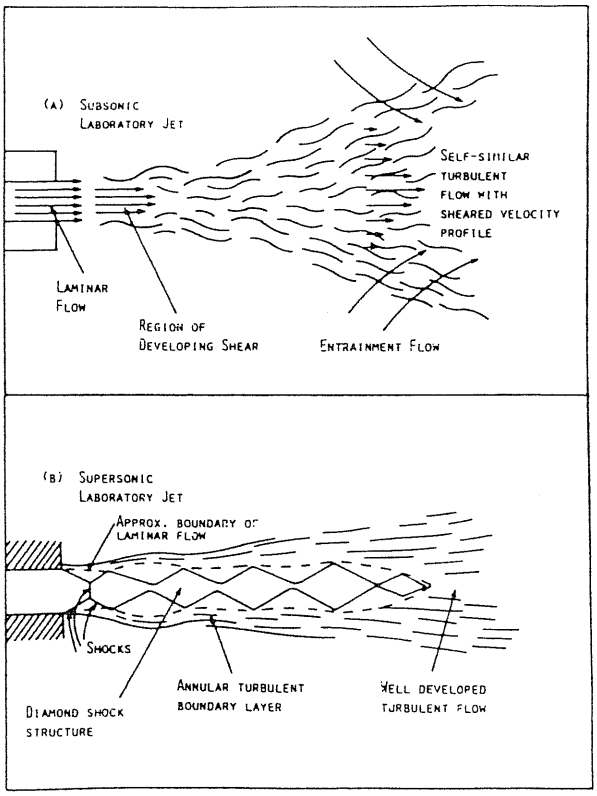

Figure 12: A schematic indication of the behaviour of subsonic and supersonic laboratory jets.

study takes advantage from some laboratory experiments on turbulent jets and shear layers (figure 11). Briefly we mention what are the major facts of these experiment relevant for astrophysical jets.

1. The Mach number dependence of the spreading rate.
2. The decrease of the spreading rate with Mach number means that it is more difficult for a supersonic jet to become fully turbulent.
3. They show some indications of why the decreasing of the spreading rate is accompanied by a decrease of the luminosity, since we reasonably expect that for higher Mach number also the source luminosity would increase.

In the regime of full turbulence the momentum of the jet diffuses laterally and the jet decelerate. At the same time also the magnetic field and the concentration of relativistic particles would diffuse laterally. Therefore a model for a turbulent jet has to be able to calculate how much deceleration is and to relate it with the above argument on the Mach number and to check its validity. The formalism to describe turbulence is based on a statistical approach (ensemble averaging), which gives a description of the mean variables of the flow. Bicknell (1986*b*) assumed a fluid dynamics description of a cylindrical jet in which the magnetic field is weak and its confinement is due to an external atmosphere. In the ensemble average formalism the density is expressed by an ensemble mean plus a fluctuating term:

$$\rho = \overline{\rho} + \rho', \quad \langle \rho' \rangle = 0 \tag{39}$$

where the brackets denote an ensemble average. For the velocity we have

$$v_\alpha = \tilde{v}_\alpha + v'_\alpha, \quad \langle \rho v'_\alpha \rangle = 0 \tag{40}$$

Substituting these terms in the classical fluid mechanics equations we obtain for the momentum and the energy

$$\frac{\partial}{\partial r}(\overline{\rho}\tilde{v}_z^2 + \frac{1}{r}\frac{\partial}{\partial r}(r\overline{\rho}\tilde{v}_r\tilde{v}_z) = -\frac{1}{r}\frac{\partial}{\partial r}(r\langle \rho v'_r v'_z \rangle) - \left(1 - \frac{\overline{\rho}}{\rho_{ext}}\right)\frac{dP}{dz} \tag{41}$$

$$\frac{\partial}{\partial z}(\overline{\rho}h\tilde{v}_z) + \frac{1}{r}\frac{\partial}{\partial r}(r\overline{\rho}\tilde{v}_r\tilde{v}_z) - \tilde{v}_z\frac{dP}{dz} = -\frac{1}{r}\frac{\partial}{\partial r}(r\langle \rho v'_r h' \rangle) + \text{dissipative terms} \tag{42}$$

where h is the specific enthalpy. The terms in the brackets are the most important in the theory of turbulence and it is not simple to obtain an expression for them at least for low Mach numbers jets. The last term in eq. (41) is the buoyancy term. The dissipative terms can be neglected in first approximation for low Mach numbers. These difficulties in obtaining an expression for the

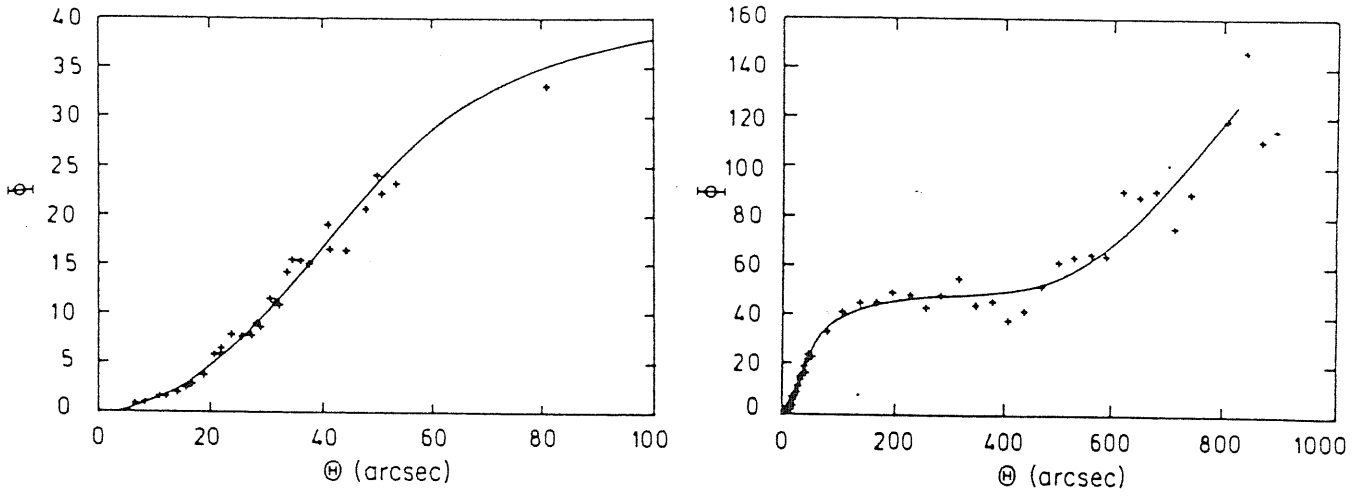

Figure 13: The FWHM (Φ) - angular distance from the core (Θ) behaviour of the jet in *NGC*315. The cross are the observational data. The curve is a spline fit to the data prescribed by the model. (From Bicknell 1986b).

turbulence terms are in part overcome through an approach based essentially on the conservation laws for the jet. With other further assumptions in which the velocity and internal pressure have a top-hat profile and with a choice of an isothermal model for the external pressure, the variations of the jet velocity, density and Mach number are derived. Bicknell (1986*a*) found that the velocity at the center of the jet has the following behaviour

$$v_c \propto p^{-3/4} R^{-2}$$

in regimes where the Mach number at the center results $M_c^2 \ll 10$. These results were applied to the spline fit of the spreading-rate data for *NGC*315 (figure 12) and the northern jet in *3C*31.

The starting idea that the delimitation between radio sources of FR I class and of FR II class can also depend on the Mach number of their jet seems to be an established fact.

3. Interaction between Relativistic Jets and Ambient Gas

3.1 Relativistic Charged Particle Interaction

The physical interaction of an highly collimated relativistic jet and the surrounding ambient gas occurs mainly through collisionless effects if the gas is sufficiently ionized. Such jets are very well collimated beams of relativistic particles. They are shown to be present in active galactic nuclei and quasars and may occur also in the nuclear region of Seyfert galaxies as observed at the VLA by Wilson and Willis (1980). The importance of this type of interaction is due to the fact that under some circumstances its by-product is represented by the significant increase of the power-law tails of electrons of the plasma background which would enhance the optical and ultraviolet line regions. Rose *et al.* (1984) investigated this phenomenon. The physics of the interaction involve some kinds of beam plasma instabilities on a small scale, typically two-stream instabilities.[1] They assumed a low density relativistic electron beam injected in a background plasma. The dimensions of the beam are such that plasma instabilities cannot grow – the time scales of the beam motioin are large enough that plasma instabilities cannot disrupt immediately the

1 The energy of the beam is lost in form of electrostatic waves and the beam is broaden in the momemtum space.

beam. Neglecting the magnetic field produced or enhanced by this interaction, the beam would heat the plasma and expand producing a plasma with lower density but with a higher temperature. The heating of the plasma may be not due to bulk heating of electrons and ions but rather due to non resonant waves which generate energetic tails in the electron velocity distribution departing from the Maxwellian distribution.[2] How significant the departure is from a Maxwellian distribution is discussed by Rose *et al.* (1987), for injected beam composed by electrons and protons and by electrons and positrons. When that gas is sufficiently dense (*i.e.* optically thick) inverse Compton scattering is the dominant loss mechanism for the beam that will result decelerated. A beam with $\gamma \approx 10^2$ will produce X-rays and low energy γ-rays.

These studied are relevant to the models of radio sources because they show the possibility for a relativistic charged beam of accelerate gas (clouds) at non relativistic velocities that are just what some radio sources models ask for, since radiation pressure alone is not a very efficient mechanism for accelerating gas.

3.2 Electromagnetic Waves in Jets: Collective Emission

Another effect concerning plasma turbulence is the case studied by Baker *et al.* (1988). They assumed that in the inner part of an astrophysical jet a beam of relativistic electrons is injected . This beam comes from the central engine. The interaction of the jet plasma with the beam drives instabilities that can have observational effects since they generate electromagnetic waves. In laboratory experiments this is a way to produce high-power radiation of short wavelengths up to 20 MW of total power within a bandwidth of ~ 40 GHz . Their model required a non relativistic plasma flow superposed by an highly beamed

2 The non-resonant plasma waves have phase velocities little greater of the bulk thermal velocity of the elctrons.

relativistic electron beam streaming parallel to the jet axis coming from the central engine. The existence of this beam can be guaranteed by a mechanism similar to that one proposed by Lovelace (1976). These beam electrons collide in a coherent way with the electrostatic waves driven by plasma turbulence. Because of their relativistic speed the radiation emitted is boosted in the forward direction and it will emerge within an angle of $\sim 1/\gamma$ with a characteristic frequency of $\approx \gamma^2 \omega_{pe}$, where ω_{pe} is the electron plasma frequency.

An interesting application of this study explains the presence of luminosity gaps in the inner region of jets in radio sources. According to Baker *et al.* (1988), collective emissions occur at a distance from the nucleus that is comparable to that observed for gaps in radio jets (this depends on the growth rates of the plasma instabilities). The coherent emission is strongly beamed and 'kills' the inchoerent synchrotron radiation, so that the former will be detectable only if the jet itself is beamed to us. At this stage such model is still too parameters dependent especially on the conditions in the plasma that drive instabilities.

Conclusions and Discussion

In this study two things have not been discussed. First the detailed mechanism of accelerating electrons at relativistic energies, that together with the magnetic field characterize the synchrotron emission. This acceleration processes are mainly identified with hot-spots in powerful radio galaxies located at the end of the jets. On the other hand we have interpreted shock structures as signatures of particles acceleration since basically a shock wave convert kinetic energy in thermal energy. To study in detail how the distribution function of the electrons changes under the effect of shocks is an entirely new problem that is not completely solved and understood. Second models of jets in compact sources (typically at VLBI scales). We only mentioned relativistic motion in the context of the velocity of jets. Jets in compact sources have been extensively reviewed by Zensus and Pearson (1986).

Throughout this study the morphological classification of Fanaroff and Riley (1974) of extragalactic radio sources has been used in discussing and modeling different properties of jets. New parameters, the Mach number M, and the density ratio, $\eta = \rho_{jet}/\rho_{ext}$, characterized the two principal regimes of jet propagation corresponding to different morphological classes. This parameter space (M,η) derived from the two restrictions that are used in numerical simulations: (a) jet and external fluid are always in static pressure balance, (b)

the system has no natural scales. Normally results are expressed in terms of units of the external density, sound speed and the sound crossing time for the beam radius. This last restriction holds if there are not significant synchrotron losses that are dynamically important. In this case an external time scale is imposed on the system.

Jets in weak radio galaxies ($P_{tot}^{1.4} < 10^{25}$ W/Hz) have a 'relaxed structure' (not well collimated) showing a transonic turbulent regime. They interact with the ambient medium mainly through entrainment. Hence they laterally expand. This regime is characterized by a competition between pressure gradients and buoyancy (which try to accelerate the jet) and entrainment (which decelerate it and increase η). Numerical simulations reproduce the global behaviour of such jets with Mach number $M \sim 2-3$, and light jet $\eta \sim 0.1$.

Jets in powerful radio galaxies ($P_{tot}^{1.4} > 10^{25}$ W/Hz) have a more streamed structure. The interaction with the ambient gas occurs mainly through shocks than entrainment. Thus they propagate more further away from the nucleus without being disrupted. Essential to this is the presence of a toroidal magnetic field generated by currents inside the jet. Numerical simulations reproduce such structure for very light jets $\eta \leq 10^{-2}$ and Mach number $M \geq 10$.

A further correlation is established: there is a critical transition in the parameter space (M, η) that correspond to the separation between FR-I class and FR-II class.

The correlation so found has its foundations in the capability of developing detailed numerical/observation comparison. This is not always possible. Infact we are basically ignorant how the synchrotron emission is related to the flow itself. To relate radio observables to the supposed flows we should compute how four Stokes parameters vary with frequency while relativistic and thermal particle densities, magnetic fields, particle energy spectra and pitch angle distributions are processed through shocks and turbulence. Moreover we

only have rough estimates on the jet composition (electrons-protons and/or electrons-positrons) and its temperature. To determine what features shown by numerical simulations are observable luminous features is the necessary question to ask before to derive any conclusion. Perhaps a more wise attitude toward numerical simulations is that of using them to investigate and to clarify the physical processes that characterized the flow rather than apply numerical simulations directly to the radio maps. There is no unified model of jets yet that account for all the morphologies observed and explains consistently the trends found.

Apart from the expected improvement of numerical computations, new insight may derive from further studies on the typical small scales plasma instabilities produced by relativistic beams interacting with the ambient. This allows a better description of the microphysics involved in jets and radio lobes. For example the filamentary structure observed in jets (*i.e.* CygnusA, M87) shows that the synchrotron emission does not 'fill' the entire volume of the jet. To calculate the distribution function for the electrons that reproduce the observed brightness distribution is a typical problem of plasma astrophysics.

Bibliography

[1] Achatz, U., Lesch, H., and R. Schlickeiser, (1990), *Astr. Ap.*, **233**, 391.

[2] Achterberg, A., Blandford, R.D., and Goldreich, P., (1983), *Nature*, **304**, 607.

[3] Adamson, T.C., Nicholls, J.A., (1959), *J. Aerospace Sci.*, **9**, 512.

[4] Baade, W., and R. Minkowski, (1954), *Ap. J.*, **119**, 215.

[5] Baker, D.N., and J.E. Borovky, G. Benford, and J.A. Eilek, (1988), *Ap. J.*, **326**, 110.

[6] Begelman, M.C., (1982), *Proc. I.A.U. Symp. 97, Extragalactic Radio Sources*, Ed. D.S.Heeschen and C.M. Wade, Dordrecht: Reidel, p.223.

[7] Begelman, M.C., Blandford, R.D., and M.J. Rees, (1984), *Rev. Mod. Phys.*, **56**, *pp*.55.

[8] Begelman, M.C., and D.F. Cioffi, (1989), *Ap. J.*, **345**, *L*41.

[9] Bicknell, G.V., (1986*a*), *Ap. J.*, **305**, 109.

[10] Bicknell, G.V., (1986*b*), *Can. J. of Phys.*, **64**, 495.

[11] Bicknell, G.V., de Ruiter, H.R., Fanti, R., Morganti, R., Parma, P., (1989), *European Southern Observatory*, Scientific Preprint no.672, Submitted to The Astrophysical Journal.

[12] Biretta, J.A., Moore, R.L., and Cohen, M.H., (1986), *Ap. J.*, **308**, 93.

[13] Blandford, R., and Rees, M.J., (1974), *M.N.R.A.S.*, **169**, 395.

[14] Blandford, R. and Königl A., (1979), *Ap. J.*, **260**, 855.

[15] Blandford, R.D., and J.E. Pringle, (1976), *M.N.R.A.S.*, **176**, 443.

[16] Blandford, R.D., and Eichler, D., (1987), *Phys. Rep.* , **154**, 1.

[17] van Breugel, W.J.M., (1980), *Astr. Ap.*, **88**, 248.

[18] Bridle, A.H., Chan, K.L., and Henriksen, R.N., (1981), *J.R.A.S. Canada*, **75**, 69.

[19] Bridle, A.H., (1982), *Proc. I.A.U. Symp. 97, Extragalactic Radio Sources*, Ed. D.S.Heeschen and C.M. Wade, Dordrecht: Reidel, p.121.

[20] Bridle,A.H., Perley, R.A., (1983), *Proc. Turin Workshop, Astrophysical Jets*, Ed. A. Ferrari and A.G. Pacholczyk, Dordrecht: Reidel, p.57.

[21] Bridle, A.H., and R.A. Perley, (1984), *Ann. Rev. Astr. Ap.*, **22**, 319,[BP].

[22] Bridle, A.H., (1984), *Astr. J.*, **89**, 979.

[23] Browne, I.W., (1983), *M.N.R.A.S.*, **204**, 23p.

[24] Burch, S.F., (1979), *M.N.R.A.S.*, **187**, 187.

[25] Burns, J.O., Gregory, S.A., and G.D. Holman, (1981), *Ap. J.*, **250**, 770.

[26] Chan, K.L., and Henriksen, R.N., (1980), *Ap. J.*, **241**, 534.

[27] Chandrasekhar, S., (1961), *Hydrodynamic and Hydromagnetic Stability*, Oxford University Press, Oxford.

[28] Cohen, M.H.,Cannon, W., Purcell, G.H., Shaffer, D.B., Broderick, J.J., Kellerman, K.I., and Jauncey, D.L., (1971), *Ap. J.*, **170**, 207.

[29] Cohn, H., (1983), *Ap. J.*, **269**, 500.

[30] De Young, D.S., (1980), *Ap. J.*, **241**, 81.

[31 Drury, L.O., (1983), *Rep. Prog. Phys.*, **46**, 973.

[32] Eilek, J.A., (1989), *Astr. J.*, **98**, 1.

[33] Falle, S.A.E.G., and M.J. Wilson, (1985), *M.N.R.A.S.*, **216**, 79.

[34] Fanaroff, B., and J.M. Riley, (1974), *M.N.R.A.S.*, **167**, 31*p*.

[35] Fanti, R., Lari, C., Parma, P., Bridle, A.H., Ekers, D., and E.B. Fomalont, (1982), *Astr. Ap.*, **110**, 169.

[36] Fanti, C., Fanti, R., de Ruiter, H.R., and Parma, P., (1987), *Astr. Ap. Suppl.*, **69**, 57.

[37] Ferrari, A., Trussoni, E., and L. Zaninetti, (1978), *Astr. Ap.*, **64**, 43.

[38] Ferrari, A., Trussoni, E., and L. Zaninetti, (1981), *M.N.R.A.S.*, **196**, 1051.

[39] Fielder, R., and T.W. Jones, (1984), *Ap. J.*, **283**, 532.

[40] Fyfe, D., Joyce, G., and Montgomery, D., (1977) *J. Plasma Phys.*, **17**, 317.

[41] Hoyle, F., Burbidge, G.R., and Sargent, W.L.W., (1966), *Nature*, **209**, 751.

[42] Kaplan, S.A., Tsytovich, V.N., (1973), *Plasma Astrophysics*, Pergamon Press, Oxford.

[43] Kellerman, K.I., and Pauliny-Toth, I., (1981), *Ann. Rev. Astr. Ap.*, **19**, 373.

[44] Krautter, A., Henriksen, R.N., and Lake, K., (1983), *Ap. J.*, **269**, 81.

[45] Laing, R.A., (1981), *Ap. J.*, **248**, 87.

[46] Landau, L.D., and E.M. Lifshitz, (1959), *Fluid Mechanics*, Pergamon Press, Oxford.

[47] Lehay, J.P., Williams, A.G., (1984), *M.N.R.A.S.*, **210**, 929.

[48] Lesieur, M., (1987), *Turbulence in Fluids*, Martinus Nijhoff Publishers, Dordrecht.

[49] Lind, K.R., Payne, D.G., Meier, D.L., and R.D. Blandford, (1989), *Ap. J.*, **344**, 89.

[50] Longair, M.S., Ryle, M., and P.A.G. Scheuer, (1973), *M.N.R.A.S.*, **164**, 243.

[51] Lovelace, R.V.E., (1976), *Nature*, **262**, 649.

[52] Margon,B., (1984), *Ann. Rev. Astr. Ap.*, **22**, 507.

[53] Marscher, A.P., and Broderick, J.J., (1982), *Ap. J.*, **255**, *L*11.

[54] Marscher, A.P., and Broderick, J.J., (1985), *Ap. J.*, **290**, 735.

[55] Miley, G.K., Heckman, T., Butcher, H., and W.J.M. van Breugel, (1981), *Ap. J. (Letters)*, **247**, *L*5.

[56] Norman, M.L., Smarr, L., Winkler, K.-H.A., and Smith, M.D., (1982), *Astr. Ap.*, **113**, 285.

[57] Norman, M.L., Smarr, L.L., Winkler, K-H.A., (1984), in *Numerical Astrophysics*, Ed. J.M. Centrella, J.M. LeBlanc, R.L. Bowers, Jones and Bartlett, Boston, p.88.

[58] Norman, M.L., Burns, J.O., and M.E. Sulkanen, (1988), *Nature*, **335**, 146.

[59] Payne, D.G., and H. Cohn, (1985), *Ap. J.*, **291**, 655.

[60] Perley, R.A., Willis,A.G., and Scott, J.S., (1979), *Nature*, **281**, 437.

[61] Perley, R.A., Bridle,A.H., Willis, A.G., (1984), *Ap. J. Supplement*, **54**, 292.

[62] Potash, R.I., Wardle, J.F.C., (1980), *Ap. J.*, **239**, 42.

[63] Rees, M., (1967), *M.N.R.A.S.*, **135**, 345.

[64] Rudnick, L.,and Edgar, B.K., (1984), *Ap. J.*, **279**, 74.

[65] Rudnick, L., (1988), *Ap. J.*, **325**, 189.

[66] Rose, W.K., Guillory, J., Beall., J.H., and S. Kainer, (1984), *Ap. J.*, **280**, 550.

[67] Rose, W.K., Beall., J.H., Guillory, J., and S. Kainer, (1987), *Ap. J.*, **314**, 95.

[68] Sanders, R.H., (1983), *Ap. J.*, **266**, 73.

[69] Synge, J.L., (1957), *The Relativistic Gas*, North Holland Pub. Co., Amsterdam.

[70] Turland, B.D., and P.A.G. Scheuer, (1976), *M.N.R.A.S.*, **176**, 421.

[71] Unwin, S.C., Cohen, M.H., Pearson, T.J., Seielstad, G.A., Simon, R.S., Linfield, R.P., and Walker, R.C., (1983), *Ap. J.*, **271**, 536.

[72] Van Dyke, M., (1982), *An Album of Fluid Motion*, The Parabolic Press, Stanford, CA.

[73] Walker, R.C., (1984), in *Physics of Energy Transport in Extragalactic Radio Sources*, Ed. by A. Bridle and J. Eilek, Green Bank, WV, p.20.

[74] Wardle, J.F.C., and Potash, R.I., (1984), in *Physics of Energy Transport in Extragalactic Radio Sources*, Ed. by A. Bridle and J. Eilek, Green Bank, WV, p.30.

[75] Weber, E.J., and L. Davis, Jr., (1967), *Ap. J.*, **148**, 217.

[76] Whitney, A.R., Shapiro, I.I., Rogers, A.E.E., Robertson, D.S., Knight, C.A., Clark, T.A., Goldstein, R.M., Marandino, G.E., Vandeberg, N.R., (1971), *Science*, **173**, 225.

[77] Wiita, P.J., (1978*a*), *Ap. J.*, **221**, 41.

[78] Wiita, P.J., (1978*b*), *Ap. J.*, **221**, 436.

[79] Willis,A.G., Strom,R.G., Bridle, A.H., Fomalont,E.B., (1981), *Astr. Ap.*, **95**, 250.

[80] Wilson, A.S., Willis, A.G., (1980), *Ap. J.*, **240**, 429.

[81] Wilson, A.S., and Ulvestad, J.S., (1987), *Ap. J.*, **319**, 105.

[82] Wilson, M.J., and S.A.E.G. Falle, (1985), *M.N.R.A.S.*, **216**, 971.

[83] Wilson, M.J., (1987*a*), *M.N.R.A.S.*, **224**, 155.

[84] Wilson, M.J., (1987*b*), *M.N.R.A.S.*, **226**, 447.

[85] Yokosawa, M., and S. Ikeuchi, and S. Sakashita, (1982), *Publ. Astron. Soc. Japan.*, **34**, 461.

[86] Zensus, J.A. and Pearson, T.J., (Editors), (1986), *Superluminal Radio Sources*, Cambridge University Press, Cambridge.